Charge transport modulation in organic electronic diodes

Fredrik Lars Emil Jakobsson

Norrköping 2008

Charge transport modulation in organic electronic diodes

Fredrik Lars Emil Jakobsson

Linköping Studies in Science and Technology. Dissertations. No. 1203

Printed by LiU-Tryck, Linköping, Sweden 2008
ISBN: 978-91-7393-830-3
ISSN: 0345-7524

Abstract

Since the discovery of conducting polymers three decades ago the field of organic electronics has evolved rapidly. Organic light emitting diodes have already reached the consumer market, while organic solar cells and transistors are rapidly maturing. One of the great benefits with this class of materials is that they can be processed from solution. This enables several very cheap production methods, such as printing and spin coating, and opens up the possibility to use unconventional substrates, such as flexible plastic foils and paper. Another great benefit is the possibility of tailoring the molecules through carefully controlled synthesis, resulting in a multitude of different functionalities.

This thesis reports how charge transport can be altered in solid-state organic electronic devices, with specific focus on memory applications. The first six chapters give a brief review of the field of solid-state organic electronics, with focus on electronic properties, resistance switch mechanisms and systems. Paper 1 and 3 treat Rose Bengal switch devices in detail – how to improve these devices for use in cross-point arrays as well as the origin of the switch effect. Paper 2 investigates how the work function of a conducting polymer can be modified to allow for better electron injection into an organic light emitting diode. The aim of the work in papers 4 and 5 is to understand the behavior of switchable charge trap devices based on blends of photochromic molecules and organic semiconductors. With this in mind, charge transport in the presence of traps is investigated in paper 4 and photochromic molecules is investigated using quantum chemical methods in paper 5.

Populärvetenskaplig sammanfattning

Elektroniska komponenter har traditionellt sett tillverkats av kisel eller andra liknande *inorganiska* material. Denna teknologi har förfinats intill perfektion sedan mitten av 1900-talet och idag har kiselkretsar mycket hög prestanda. Tillverkningen av dessas kretsar är dock komplicerad och är därför kostsam. Under 1970-talet upptäcktes att *organiska* polymerer (*dvs* plast) kan leda ström under vissa förutsättningar. Genom att välja lämplig polymer och behandla den med vissa kemikalier (så kallad dopning) kan man variera ledningsförmågan från isolerande till nästintill metallisk. Det öppnar möjligheten för att skapa elektroniska komponenter där dessa organiska material utgör den aktiva delen istället för kisel. En av de stora fördelarna med organiska material är att de vanligtvis är lösliga i vanliga lösningsmedel. Det gör att komponenter kan tillverkas mycket enkelt och billigt genom att använda konventionell tryckteknik, där bläcket har ersatts med lösningen av det organiska materialet. Det gör också att komponenterna kan tillverkas på okonventionella ytor såsom papper, plast eller textil. En annan spännande möjlighet med organiska material är att dess funktioner kan skräddarsys genom välkontrollerad kemisk syntes på molekylär nivå. Inom forskningsområdet *Organisk Elektronik* studerar man de elektroniska egenskaperna i de organiska materialen och hur man kan använda dessa material i elektroniska komponenter.

Vi omges idag av apparater och applikationer som kräver att data sparas, som till exempel digitala kameror, datorer och mobiltelefoner. Eftersom det finns ett stort intresse från konsumenter för nya smarta produkter ökar behovet av mobila lagringsmedia med stor lagringskapacitet i rasande fart. Detta har sporrat en intensiv utveckling av större och billigare fickminnen, hårddiskar och minneskort. Många olika typer av minneskomponenter baserade på organiska material har föreslagits de senaste åren. I vissa fall har dessa påstått kunna

erbjuda både billigare och större minnen än vad dagens kiselteknologi tillåter. En typ av organiska elektroniska minnen baseras på en reversibel och kontrollerbar förändring av ledningsförmågan i komponenten. En informations enhet – en så kallad *bit* – kan då lagras genom att till exempel koda en hög ledningsförmåga som en ”1” och en låg ledningsförmåga som en ”0”. Den här doktorsavhandlingen är ett försök till att öka förståelsen för sådana minneskomponenter.

Minneskomponenter bestående av det organiska materialet Rose Bengal mellan metallelektroder har undersökts. Egenskaper för system bestående av många sådana komponenter har beräknats. Vidare visas att minnesfenomenet inte härstammar i det organiska materialet utan i metallelektroderna. Tillsammans med studier av andra forskargrupper har det här resultatet bidragit till en debatt om huruvida minnesmekanismerna i andra typer av komponenter verkligen beror på det organiska materialet.

Olika sätt att ändra transporten av laddningar i organiska elektroniska system har undersökts. Det visas experimentellt hur överföringen av laddningar mellan metallelektroder och det organiska materialet kan förbättras genom att modifiera metallelektroderna på molekylär nivå. Vidare har det studerats teoretiskt hur laddningar kan fastna (så kallad *trapping*) i organiska material och därmed påverka ledningsförmågan i materialet.

En speciell typ av organiska molekyler ändrar sin struktur, och därmed egenskaper, reversibelt när de belyses av ljus av en viss våglängd, så kallade *fotokroma* molekyler. Denna förändring kan användas till att ändra ledningsförmågan genom en komponent och därmed skulle man kunna använda molekylerna i en minneskomponent. I den sista delen av avhandlingen används kvantkemiska metoder för att beräkna egenskaperna hos dessa molekyler för att öka förståelsen för hur de kan användas i minneskomponenter.

Acknowledgements

The path to a PhD is not always an easy one. There were dark times when I really questioned what I was doing. And there were good times of exciting scientific discovery that made me understand why I was doing it. In those moments, all the hard work was rewarded by the satisfaction of understanding and the relief that the work had not been in vain. Sometimes these sparks of understanding resulted in a bitter sweat and complete rethinking of my research. At other times it gave me the full joy of having "the flow" and being successful.

A very important part of research is the communication with others – in discussions with supervisors and colleagues as well as communications with the rest of the research community at conferences and within external collaborations. And of course a very important part of any great endeavor is the support of all important people – friends and loved ones – in your life. This thesis would never have been written if it were not for all these fantastic people. So before you read the rest of the thesis (which of course you will do…) I would like to take the opportunity to mention a few of those fantastic people that have helped me reach the end of this road.

I would first like to thank Professor Magnus Berggren for giving me the opportunity to work and study in such a great environment and for your never-ending optimism. Thank you Xavier Crispin for your enthusiasm that made me carry on through the darkest of lab hours and for being a great supervisor. I am very grateful to Sophie Lindesvik for all practical help and for bailing me out from tricky administrative situations more than once. I would like to thank the other members – past and present – of the Organic Electronics research group (Daniel, David, Edwin, Elias, Elin, Emilien, Georgios, Hiam, Isak, Joakim, Klas, Kristin, Lars, Linda, Maria, Max, Nate, Oscar, Payman, PeO, Peter, Xiangjun, Yu) for creating a stimulating and joyful environment at work. I have had the pleasure of being part of the Center of Organic Electronics (COE) and would

therefore like to thank everybody within COE (Abay, Kristofer, Lasse Stefanz, Linda, Mahiar, Mattias, Olle, Robert, Slawomir and everybody else) for many stimulating discussions within the field of organic electronics and other less scientific – but just as fun – activities. My experimental work would not have been possible if it were not for the great technical support and advice from Bengt Råsander and Lasse Gustavsson. Both of you have saved my experiments more than once by knowing the nuts and bolts of everything in the lab.

My work to discover the truth about Rose Bengal devices took me to Philips Research Laboratories in Eindhoven, the Netherlands. I would like to sincerely thank Dago de Leeuw for giving me the opportunity to come to his lab and for all the help from the great people at Philips (Michael C, Michael B, Edsger, Frank and everybody else).

A rainy Tuesday in January I left Linköping for a stay in Mons, Belgium. I would like to kindly thank Professor Roberto Lazzaroni for hosting me. A special thanks to my quantum chemistry guru Philippe Marsal for tolerating four weeks of continuous questions. I would also like to thank everybody (David, Jérôme, Lucas, Mike, Patrick, Said, Yoanne and everybody else) for giving me an unforgettable time in Mons and for giving me the insights of Belgian beers.

But the journey to this dissertation was not only hard work. A big hug to all my great friends – you know who you are – for all the laughs in good times and support in bad times.

Thanks to my dear father and mother – Lars and Karin – and to my sister with family – Johanna, Mikael and little Elsa – for all the support and for always being there.

Last, but not least, I would like to thank Louise, the love of my life. Without your love, wisdom and patience I would never have made it.

Related papers

Papers included in this thesis

Paper 1: Towards addressable organic impedance switch devices

F. L. E. Jakobsson, X. Crispin, M. Berggren

Applied Physics Letters **87** (2005) 063503

Paper 2: Towards all-plastic flexible light emitting diodes

F. L .E. Jakobsson, X. Crispin, L. Lindell, A. Kanciurzewska, M. Fahlman, W. R. Salaneck, M. Berggren

Chemical Physics Letters **433** (2006) 110-114

Paper 3: On the switching mechanism in Rose Bengal-based memory devices

F. L. E. Jakobsson, X. Crispin, M. Cölle, M. Büchel, D. M. de Leeuw, M. Berggren

Organic Electronics **8** (2007) 559-565

Paper 4: Prediction of the current versus voltage behavior of devices based on organic semiconductor host-guest systems

F. L. E. Jakobsson, X. Crispin, M. Berggren

Submitted

Paper 5: Tuning the energy levels of photochromic diarylethene compounds for optoelectronic switch devices

F. L. E. Jakobsson, P. Marsal, S. Braun, X. Crispin, J. Cornil, M. Fahlman, M. Berggren

Manuscript

Related papers not included in this thesis

The Origin of the High Conductivity of Poly(3,4-ethylenedioxythiophene)-Poly(styrenesulfonate) (PEDOT-PSS) Plastic Electrodes

X. Crispin, F. L. E. Jakobsson, A. Crispin, P. C. M. Grim, P. Andersson, A. Volodin, C. van Haesendonck, M. Van der Auweraer, W. R. Salaneck, M. Berggren

Chemistry of Materials **18** (2006) 4354-4360

Transparent, Plastic, Low-Work-Function Poly(3,4-ethylenedioxythiophene) Electrodes

L. Lindell, A. Burquel, F. L. E. Jakobsson, V. Lemaur, M. Berggren, R. Lazzaroni, J. Cornil, W. R. Salaneck, X. Crispin

Chemistry of Materials **18** (2006) 4246-4252

Intrinsic and extrinsic influences on the temperature dependence of mobility in conjugated polymers

L. M. Andersson, W. Osikowicz, F. L. E. Jakobsson, M. Berggren, L. Lindgren, M. R. Andersson, O. Inganäs

Organic Electronics, in press

Contents

Part 1:

The introduction

Chapter 1

Introduction to organic electronics

Since the advent of electronics the semiconductor industry have been dominated by silicon and similar inorganic semiconductors. Today, silicon circuits are taken for granted in our lifestyle and we find them in everyday appliances such as TVs, computers, mobile phones and even electrical razors. In this context, plastic materials have traditionally served as passive components, such as insulators, as electronics-carrying substrates or in packaging.

On November 23, 1976, something happened that changed the role of organic materials within the field of electronics [1]. In a lab at Pennsylvania State University, Alan J. Heeger, Alan G. MacDiarmid and Hideki Shirakawa made an astonishing discovery. When treated with bromine the conductivity of polyacetylene, an organic polymer, was changed by seven orders of magnitude, resulting in a conductivity close to being metallic in its character [2]. According to Shirakawa's own accord the conductivity increased so rapidly and radically that the expensive measurement equipment was destroyed [1]. Heeger, MacDiarmid and Shirakawa were awarded the year 2000 Nobel Prize in chemistry "for the discovery and development of conductive polymers". This opened up the opportunity for organic polymers as the active material in electronic applications.

The basic components of organic materials are carbon and hydrogen atoms. Commonly, these compounds also contain other atomic species such as phosphor, iodine, bromide, nitrogen, oxygen and sulfur. Organic compounds are abundant around us. In fact all living organisms – from the simplest bacteria to the complex human – are all made up of organic materials. Organic electronics is the art of making electronic components from organic-, i.e. carbon based, compounds.

In the three decades since the discovery of conducting polymers the field of organic electronics has gone from a curiosity in the research lab, to the brink of commercialization. Organic light emitting diodes are already on the market in simple applications and high-end displays are forecasted to reach the market within the very near future.

Traditional inorganic electronics is commonly produced using complicated and utterly expensive processing methods, requiring both high-class clean room facilities and advanced vacuum equipment. One of the very appealing possibilities with organic materials is that they can be processed from solution. This enables several very cheap production methods, in the same way as ink is deposited on paper, and opens up the possibility to use unconventional substrates, such as flexible plastic foils. Even paper has emerged as a viable carrier for organic devices [3]. This evolution has at least partly been boosted by the interest from the paper and packaging industry to improve the value of their products in the world of internet and the "paperless" office.

Organic compounds are not only interesting for very low-end and cheap applications. By carefully controlling the synthesis of the organic molecule it is possible to tailor its functionality. This is very interesting for nano-applications, were devices are made of a small numbers of molecules or even a single molecule. In this way molecular switches [4] as well as motors [5] have been realized. Molecules can also be designed to automatically assemble into well defined larger structures, so called self-assembly [6]. This could greatly facilitate the fabrication of potentially very complex nano systems, consisting of single-molecule devices.

This thesis reports how charge transport can be altered in organic devices. This is done from both a dynamic perspective, as in resistance switch devices, and from a static perspective, as in the modification of electrode properties to improve charge injection. The first six chapters give a brief review of the field of solid-state organic electronics. In chapter 2, the fundamental physics of organic materials is discussed and in chapter 3 the charge transport processes are treated. Chapter 4 gives an introduction to some of the important resistance switch phenomenon in organic materials while chapter 5 and 6 discuss how

organic materials can be used in devices and how these can be combined into larger system.

Paper 1 and 3 treat Rose Bengal switch devices in detail – how to improve these devices for use in cross-point arrays (paper 1) and the origin of the switch effect (paper 3). Paper 2 investigates how the work function of a conducting polymer can be modified to allow for better electron injection into an organic light emitting diode. In paper 4, I discuss how charge transport is affected by the presence of traps. In paper 5, properties relevant for charge transport for photochromic molecules is investigated using quantum chemical methods. The aim of the work in papers 4 and 5 is to understand the behavior of switchable charge trap devices based on blends of photochromic molecules and organic semiconductors.

Chapter 2

Properties of conjugated materials

All materials are made up of atoms, with a positively charged nucleus surrounded by electrons carrying a negative charge. The properties of the material originate in how these atoms are connected and how the nucleus and the electrons interact with surrounding atoms. The electron distribution in the atom determines how bonds are formed with other atoms, resulting in molecules or solids with different properties than the isolated atom. The electronic distribution also determines to a large extent the optical and electrical properties of the material.

The electrons in an atom are described by quantum mechanical wave functions, $\Psi(\mathbf{r},t)$, called atomic orbitals. These wave functions are solutions to the Schrödinger equation in the electrical potential of the positive nuclei and the surrounding negative electrons [7]. The energy of the electrons is given by the eigenvalues of the equation and the orbitals of the eigenfunctions. According to quantum mechanics the square of the modulus of the wave function, $|\Psi(\mathbf{r},t)|^2$, of an occupied orbital gives the probability of finding the electron at the position $\mathbf{r}$ at time t. $\Psi(\mathbf{r},t)^2$ falls of rapidly for position $\mathbf{r}$ further away from the nucleus. For atoms in their most stable state (i.e. ground state), the wave function is stationary ($\Psi = \Psi(\mathbf{r})$), meaning that the potential felt by the electrons is time independent. Since the electron is a charged particle the orbital also describes the charge density of the occupied orbital. The spatial atomic orbitals are uniquely identified by a set of quantum numbers – the principal quantum number, n, and two numbers related to the orbital angular momentum, l and m. For historical reasons the values of l is commonly denoted s, p, d, f etc. In figure 2.1 the first few atomic orbitals are shown. Electrons also possess an intrinsic angular

momentum called spin. Because the spin quantum number for electrons is half-integer they follow the Pauli principle. In other words only two electrons can occupy the same orbital, and those two electrons must have different spin states (up and down).

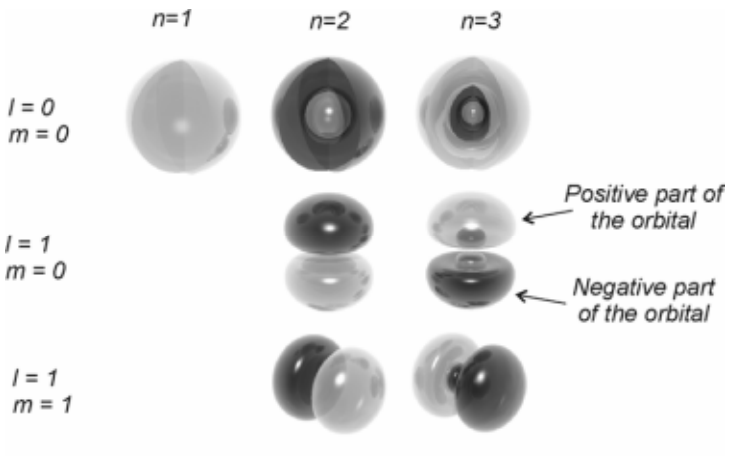

Figure 2.1: The first few s- and p-orbitals. Bright and dark marks the regions of positive and negative wave functions respectively.

When two atoms come close, they might form bonds and merge into a molecule, due to interaction of the outer electronic orbitals. Depending on the sign and shape of the atomic orbitals the character of the bond will be different. The valence electrons in the combined system are attracted simultaneously by the two nuclei. Consequently they are described by new wave functions, called molecular orbitals, resulting from the constructive or destructive interference of the atomic orbitals (see figure 2.2). If the orbitals interfere constructively the resulting molecular orbital will be non-zero between the nuclei, resulting in a finite probably of finding an electron there. Consequently there will be a negative charge density between the positive nuclei, resulting in an attraction between the atoms with the electrons acting as glue. These are called bonding molecular orbitals, since they promote bonding between the atoms. On the contrary, if the

atomic orbitals interfere destructively, there is no probability to find the electrons between the two atoms. With no negative charge density present, the positive nuclei will repel each other. Therefore these kinds of orbitals are called anti-bonding orbitals, and have a higher energy than the bonding orbitals.

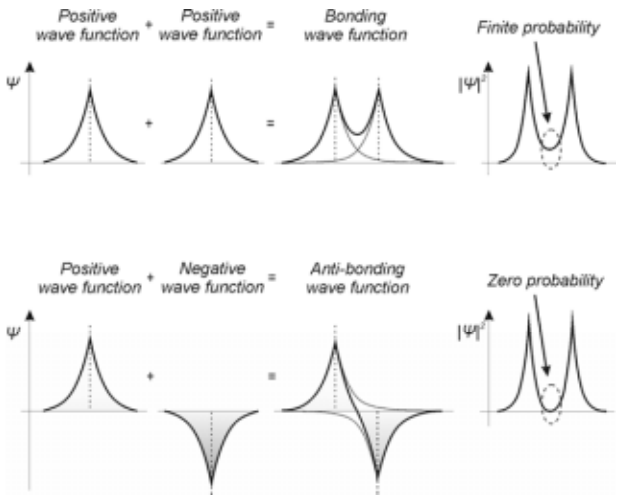

Figure 2.2: The formation of bonding and anti-bonding wave functions of two atoms with 1s outer orbitals.

In an energy diagram, the formation of bonding- and anti-bonding orbitals appears as a splitting of the atomic single energy level into two molecular energy levels. The anti-bonding molecular orbital is destabilized (pushed upwards), while the bonding molecular orbital is stabilized (pushed down). The energy separation between those two orbitals indicates the strength of the interaction between the atomic orbitals. As an example, let's consider the formation of bonds between hydrogen atoms. One hydrogen atom has one electron. If two atoms are close to each other, they form the dihydrogen molecule, H_2, characterized by split HOMO and LUMO levels. Now, if two dihydrogen molecules are put close to each other on a line to form a "dimer", the HOMO and LUMO split into two levels and four molecular orbitals are created. When two dimers are in close contact the

dimerized energy levels now split again and eight molecular orbitals are formed. This process can be extrapolated to an infinite chain of dihydrogen molecules for which the energy difference between orbitals becomes vanishingly small. In this case one can speak about a band instead of discrete energy levels to describe this one-dimensional solid. The case of two- or three-dimensional solids can be treated analogously. The width of the band, W, is determined by how strong the coupling between the atomic orbitals is. The stronger the coupling the more the energy levels will be split and hence the wider the band. The band formed from occupied orbitals is called valence band, the band created from unoccupied orbitals is called the conduction band. Such electronic band diagram is typical of semiconductors and insulators. Splitting of energy levels and formation of bands are shown for a series of carbon based compounds in figure 2.3

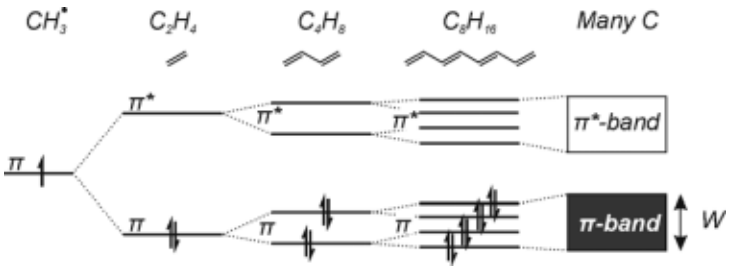

Figure 2.3: As two atoms bonds together, into a dimer, the molecular levels are split into bonding and anti-bonding levels. As several dimers are bound together the splitting of the HOMO and LUMO levels continues. In the limit of very large number of dimmers bands are formed.

In the ground state of a molecule, the electrons occupy the set of allowed molecular orbitals that give the lowest energy for the molecule. The orbital that is occupied with the highest energy is called the Highest Occupied Molecular Orbital (HOMO) and the next higher orbital is called the Lowest Unoccupied Molecular Orbital (LUMO). The chemistry and physics of molecules are to a large extent determined by the HOMO and LUMO levels. For solids, the top of the

valence band and the bottom of the conduction band determine to a large extent the optical properties and charge transport features of semiconductors.

2.1 Bonds

The type of bond described above is called *covalent bonds*. Two other types of bonds are ionic- and van der Waals bonds. In a covalent bond, if the electronegativity of the atoms differs, the electronic charge distribution will tend towards the more electronegative atom. This will cause a charging of the atoms with opposite polarity, resulting in additional columbic attraction and a dipole along the bond axis. If the electronegative difference between two atoms is large, an electron is completely transferred to the more electronegative atom. In this case the major contribution to the bond strength is electrostatic and the bond is called an *ionic* bond. If the charge transfer is incomplete the bond becomes a combination of both covalent and ionic, a so-called polar covalent bond.

Intermolecular interactions are of various origins: interactions between (induced) dipoles and (induced) dipoles, or interactions between (induced) dipoles and charges. Those interactions are grouped under the name *Van der Waals* bonds and are very weak and easily broken. For some molecules, other bonding mechanisms become important, such as hydrogen bonds in alcohols. Hydrogen bonds are stronger than Van der Waals interactions. In molecular solids atoms within molecules are bound together by rather strong covalent or ionic bonds. Molecules on the contrary are bound to the surrounding molecules by weak Van der Waals bonds.

2.2 Hybridization

In the case of organic materials the backbone of the molecule consists of carbon atoms, bond together by covalent bonds. An isolated carbon atom has six electrons and its ground state configuration is $1s^2 2s^2 2p^2$. Depending on the potential created by the surrounding atoms, the wave function of the valence

electrons is distorted and can be described with hybridized orbitals. In the methane molecule, CH_4, four hydrogen atoms are surrounding the carbon atom. In that case, the four electrons in the outer shells form four covalent σ-bonds with neighboring hydrogen atoms. Those four electrons are described by four equivalent hybrid orbitals, so-called sp^3 hybrid orbitals that can be found as a linear combination of one 2s-orbital and three 2p-orbitals. The sp^3-orbitals form a tetrahedral structure with an angle of approximately 109º between the orbitals. In ethylene, $H_2C=CH_2$, three out of four electrons in the outer shells of one carbon atom adopt a wave function called sp^2-hybrid orbital originating from a combination of one s-orbital with only two p-orbitals. The remaining electron is described by one unperturbed p-orbital. This configuration is called sp^2-hybridization with the sp^2 orbitals in the same plane with 120º between the orbitals, while the p-orbital is perpendicular to the rest of the orbitals. In ethylene, two of the sp^2-hybridized orbitals interact with the 1s orbital of hydrogen to form two σ(C-H)-bonds. The two remaining sp^2-hybridized orbitals form a σ(C-C)-bond, while the unmodified p-orbitals form a π(C=C)-bond. This extra bond between the two carbon atoms appears as a double bond (C=C) in the chemical notation. The sp^3- and sp^2 hybridization is shown in figure 2.4

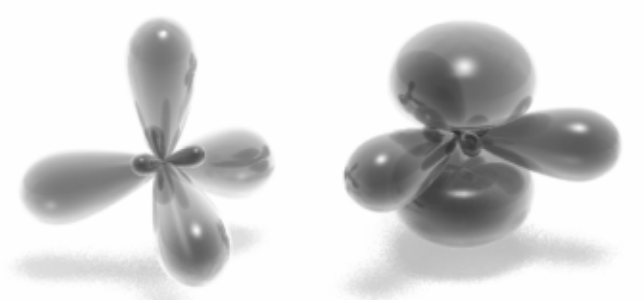

Figure 2.4: sp^3- (left) and sp^2- (right) hybridized orbitals.

2.3 Conjugation and Peierl's instability

A conjugated molecule has a skeleton formed by three or more adjacent atoms carrying a p-orbital. Those p-orbitals interact and form π-bonds pointing perpendicularly to the plane of the σ-bonds. Conjugated molecules are characterized by an alternation between double and single bonds along their skeleton. The p-orbitals of many atoms interact and form delocalized molecular orbitals that stabilize the molecule. As an example, butadiene (H_2C=CH-CH=CH_2) is one of the smallest conjugated molecules and displays an alternation between double and single bonds in the carbon-based skeleton.

Very long chains of conjugated molecules are called conjugated polymers, for instance trans-polyacetylene (figure 5.1). Even for such long chains, it turns out that the lowest energy of the system is not when the π-orbitals interacts equally with the carbon atoms on both sides. Instead a slightly shorter distance (1.34 Å) to one of the neighbors at the expense of a slightly longer distance (1.47 Å) to the other neighbor is favored energetically. This dimerization is called the Peierl's distortion, and it is the origin of the semiconducting properties of trans-polyacetylene, characterized by an energy gap between the valence and the conduction band. If the bonds would be equally long throughout the polymer chain, the energy gap between conduction and valence bands would disappear, resulting in a one-dimensional metal. A few examples of conjugated molecules are shown in figure 5.1.

2.4 Optical properties

When a molecule absorbs a photon of sufficient energy, the photon energy is given to the electrons and the electron density rearranges in space. Since the nucleus is much heavier than the electrons, the electronic excitation process (~10^{-15}-10^{-16}s) is much faster than the geometrical relaxation time of the molecule (~10^{-14}-10^{-13}s). Hence, the electronic excitation takes place without a change in the molecular structure, a so-called vertical transition (see figure 2.5). Due to this vertical transition, the photon energy is transferred to the electrons and to the

nuclei. The additional nuclei energy is in the form of vibrational motion, while the additional electronic energy is related to the changes in electron density. In a single-electron picture, this electronic energy increase can be explained approximately as follows: one electron in the HOMO becomes excited to the LUMO upon light absorption. For this reason the molecule is excited to a vibrational excited state of the electronic excited state, see figure 2.5. The anti-bonding character of the LUMO results in an overall reduction of bond strength, when it is occupied. Consequently the relative position of the nuclei changes after the excitation.

The excited molecule strives to return to its ground state via various relaxation processes. In the single-electron picture, this is equivalent to the electron in the LUMO comes back to the HOMO. Since the lifetime of the excited electronic state is long, the molecule first relaxes down to the vibrational ground state of the excited electronic state. Relaxation down to the electronic ground state can either be through formation of heat (non-radiative decay, also called quenching), or by the emission of a photon, the latter called *photoluminescence*. Note that the emitted photon has a lower energy than the excitation photon, the difference called Stokes shift.

In a single-electron picture, upon excitation of the molecule a hole is left in the HOMO when the electron is excited to the LUMO. Since the hole is positive and the electron is negative, there will be a columbic attraction between the two charges – they form a bound electron-hole pair called an exciton and characterized by an exciton binding energy. The exciton is an uncharged particle in a molecular solid that can travel. Since it does not carry an effective charge, it does not migrate in an electric field, although it might diffuse due to concentration gradients. The onset energy for absorption (i.e. the optical gap) differs from the HOMO-LUMO gap with the exciton binding energy:

$$h\nu = E_{LUMO} - E_{HOMO} - E_{be} \tag{2.1}$$

where E_{be} is the binding energy of the exciton. Typical value of exciton binding energy in organic semiconductors is 0.3 eV [8].

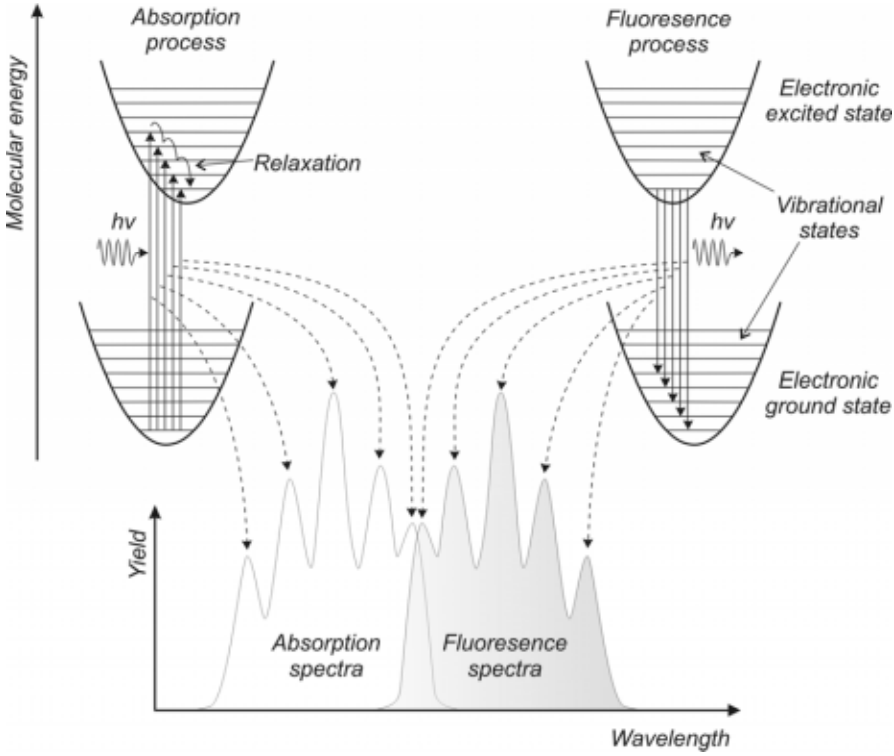

Figure 2.5: Absorption and fluorescence processes in organic materials [9].

Excitons are not only formed within a molecule upon optical excitation. In a molecular solid, when a hole and an electron come into close vicinity columbic attraction might lead to the formation of an exciton, even if they do not originate from the same molecule. This can be utilized by injecting electrons and holes from opposing contacts to the material and making them form excitons and recombine, a process called *electroluminescence*. According to quantum mechanics, the optical transition conserves the spin. Since most conjugated materials have a singlet ground state, this implies that the exciton can only recombine radiatively if it is a singlet excited state. Such states correspond to an electronic configuration with the electron in the HOMO and the electron in the LUMO having opposite spin. If those two electrons have the same spin, the

exciton is called a triplet. Unfortunately, according to spin statistics only 25% of the excitons formed by injected charges are singlets, setting an upper level for electroluminescent efficiency. In reality it turns out that triplet excitons can recombine radiatively under certain circumstances, but with a lower probability. This process is called *phosphorescence* and is a very slow and low-intensity process.

2.5 Charge carriers

Because of the strong electron-structure coupling, the relevant charge carriers in organic materials are in general not seen as an electron or hole but rather as their charge together with the resulting lattice distortion. This distortion can be described as a soliton, a polaron or a bipolaron depending on the chemical nature of the conjugated molecules or polymers [10].

Some molecules have a degenerate ground state, i.e. there exists more than one ground state conformation with the same energy. An example of such a polymer is trans-polyacetylene, which in the ground state have two equivalent ways of arranging the single- and double bond alteration. Polymer chains with odd number of carbon atoms contain a π-electron that is located between two domains of opposite bond length alternation. The interface between the two phases is not clear-cut but will extend over several bonds. This unpaired electron together with the extended bond distortion is called a soliton, and has been found to be the relevant charge carriers in trans-polyactylene [11]. Since molecules with degenerate ground state are rare, solitons are only of interest in a few occasions. The energy levels and allowed optical transitions of the soliton are shown in figure 2.6.

Most of the conjugated molecules and polymers have a non-degenerate ground state. That is if one changes the bond length alternation, the energy of the system changes. In such materials, when an extra electron or hole is present, the molecular structure is locally changed such that a local modification in the bond length alternation is introduced. The charge (electron or hole) together with

this surrounding relaxed structure is called a (negative or positive) polaron. The level of lattice distortion, i.e. the binding energy of the polaron, depends on how strongly the electron couples to the molecular structures. The lattice relaxation can extend over several molecular units, especially in polymers where the monomers are strongly coupled along the polymer chain. Therefore polarons are delocalized over several monomeric units in polymers. In some polymers, at moderate- to high carrier concentrations, two polarons can bind together to from a more stable structure called a bipolaron. The energy levels and allowed optical transitions for polarons and bipolarons are shown in figure 2.7.

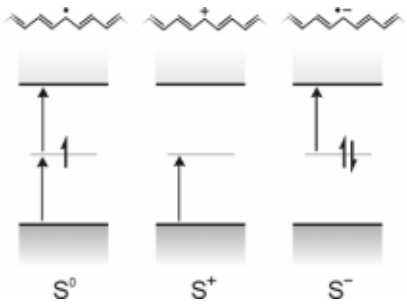

Figure 2.6: The allowed energy levels and optical transitions of a neutral soliton (S^0), a positively charge soliton (S^+) and a negatively charged soliton (S^-).

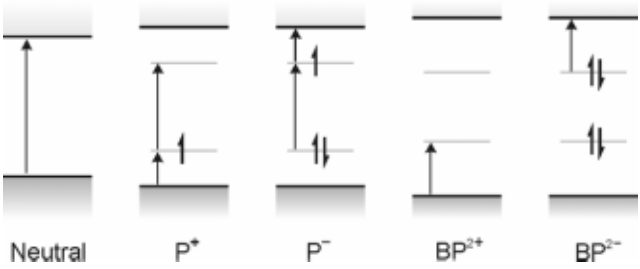

Figure 2.7: The energy levels and allowed optical transitions for a neutral molecule, a positively and negatively charged polaron (P^+ and P^-) and a positively and negatively charged bipolaron (BP^+ and BP^-).

2.6 Doping

The electrical conductivity of organic materials can be varied in a wide range by adding (n-doping) or removing (p-doping) electrons, figure 2.8. In chemical terms the doping process can be regarded as a redox reaction where the removal of an electron is called oxidation and the addition of an electron is called reduction. In the case of p-doping (n-doping) the host molecule is oxidized (reduced), resulting in a positively (negatively) charged polaron balanced in its vicinity by a negatively (positively) charged anion (cation). Doping can be achieved via two distinct processes: chemical and electrochemical doping.

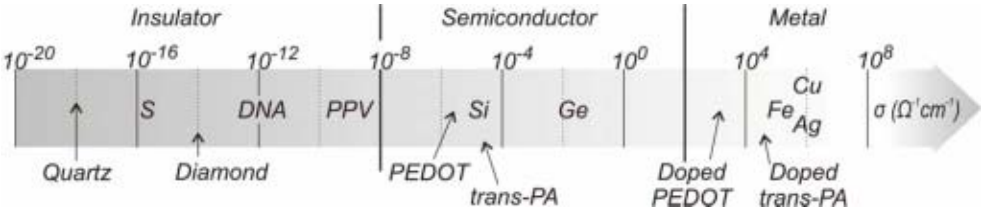

Figure 2.8: Conductivity of some organic- and inorganic materials. The conductivity of some organic materials can be altered by many orders of magnitude upon doping.

In case of chemical doping, the dopant must have energy levels in such a way that charge transfer is promoted between the host- and the dopant molecule, see figure 2.9. If the HOMO of the dopant molecule is close to the LUMO of the host molecule, an electron can easily be transferred, forming a negative polaron that can contribute to charge transport. In this case the material becomes n-doped and the molecule in this case is called a donor. The other alternative is that the LUMO of the dopant molecule is close to the HOMO of the host molecule. In this case an electron can easily be transferred to the dopant molecule, yielding a vacant state (a hole) in the host molecule that transforms into a positive polaron. The dopant is called an acceptor molecule and the host molecule can be regarded as p-doped.

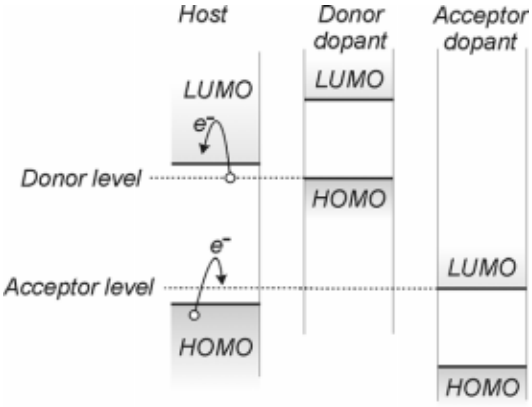

Figure 2.9: A material (host) can become p-doped by species with LUMO close to the HOMO of the host. In the same way it can become n-doped by species with HOMO close to the host LUMO.

Electrochemical doping requires the presence of an electron- and an ion reservoir. An electron is transferred between the organic material and the electron reservoir due to an applied potential difference. After electron transfer, polarons in the molecular material are balanced by an ion of opposite charge from the ion reservoir. Electrochemistry offers a convenient way for dynamic doping/dedoping in a device [12]. In its simplest form the organic film is exposed to an electrolyte (ion reservoir) and an electrical potential is applied between the film and a counter electrode (electron reservoir). In the case of the widely used PEDOT:PSS this can be expressed with the following reaction:

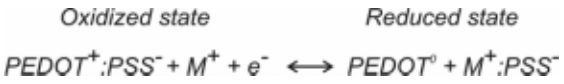

When PEDOT is oxidized polarons and subsequently bipolarons are formed, creating states in the band gap. This results in lower energy optical transitions and consequently absorption in the IR-region.

2.7 Calculating molecular properties

Solving the Schrödinger equation for anything but the simplest molecule is a formidable task. Although the Born-Oppenheimer approximation [7] offers a way to separate the molecular wave function into an electronic part and a nuclear part, the interaction between electrons still offers a great challenge. A computational efficient method to solve this problem is based on the Density Functional Theory (DFT) proposed by Hohenberg and Kohn [13-16]. This theory is attractive since, in principle, the energy of an electronic system is given by a functional, E[ρ(**r**)] of the electronic density ρ(**r**). All properties of the ground state of an n-electron system can be obtained from a simple 3-variable function: the electronic density. However, in order to determine the electronic density from the variation principle, the electron density needs to be expressed from n monoelectronic orbitals $\Psi_i(r)$ [17] :

$$\rho(\mathbf{r}) = \sum_{i=1}^{n} |\Psi_i(\mathbf{r})|^2 \qquad (2.2)$$

Kohn and Sham [18] found a self-consistent method to solve the problem, transforming it from the case of a system of interacting electrons into the case of non-interacting electrons in an effective potential. Expressed in terms of wave functions, calculating the ground state of the molecule is a $3n$-dimensional problem – 3 spatial dimensions for each n electronic wave function.

Let us assume a system of non-interacting electrons in an effective potential of V_{eff}. Then, the energy functional of this system can be defined as

$$E[\rho(\mathbf{r})] = T[\rho(\mathbf{r})] + \int V_{eff}(\mathbf{r})\rho(\mathbf{r})d\mathbf{r} \qquad (2.3)$$

where T gives the kinetic energy of the electrons. The ground state of the system is given by the ρ(**r**) that minimizes (2.3) under the condition that the total number of electrons is n ($i.e. \int \rho(\mathbf{r})d\mathbf{r} = n$). Using the Lagrange method, the minima is found by the functional derivative of the energy, given by:

$$\frac{\delta E[\rho(\mathbf{r})]}{\delta\rho(\mathbf{r})} = \frac{\delta T[\rho(\mathbf{r})]}{\delta\rho(\mathbf{r})} + V_{eff}(\mathbf{r}) = \mu \tag{2.4}$$

where μ is a Lagrange multiplier that assures that the total number of electrons is *n*. On the other hand, it is straightforward to find the ground state wave functions, ψ_i, of a system with non-interacting electrons through the Schrödinger equation [7], in this particular case given by:

$$\left(-\frac{1}{2}\nabla_i^2 + V_{eff}(\mathbf{r})\right)\psi_i(\mathbf{r}) = \varepsilon_i\psi_i(\mathbf{r}) \tag{2.5}$$

In other words, this set of ψ_i gives the $\rho(\mathbf{r})$ that minimizes (2.3) through (2.2).

Assume now that the electrons are interacting and that the position of the nuclei are known and given by an external potential V_{ext}. The energy of the system can then be defined as:

$$E[\rho(\mathbf{r})] = T[\rho(\mathbf{r})] + \int V_{ext}(\mathbf{r})\rho(\mathbf{r})d\mathbf{r} + \frac{1}{2}\int \Phi(\mathbf{r})\rho(\mathbf{r})d\mathbf{r} + E_{xc}[\rho(\mathbf{r})] \tag{2.6}$$

where the second term gives the energy due to the interaction of the electrons with the external potential generated by the nuclei and the third term gives the classical Coulomb interaction of $\rho(\mathbf{r})$. The last term, E_{xc}, is commonly called the exchange-correlation functional and contains the correction to the energy due to the non-classical nature of the electrons. The ground state of the system is again found by minimizing the energy under the condition that the total number of electrons is *n*, *i.e.*

$$\frac{\delta E[\rho(\mathbf{r})]}{\delta\rho(\mathbf{r})} = \frac{\delta T[\rho(\mathbf{r})]}{\delta\rho(\mathbf{r})} + V_{ext}(\mathbf{r}) + \Phi(\mathbf{r}) + \frac{\delta E_{xc}[\rho(\mathbf{r})]}{\delta\rho(\mathbf{r})} = \mu \tag{2.7}$$

Comparing (2.7) and (2.4) it is clear that the two problems are identical if the effective potential is defined as:

$$V_{eff} = V_{ext}(\mathbf{r}) + \Phi(\mathbf{r}) + \frac{\delta E_{xc}[\rho(\mathbf{r})]}{\delta\rho(\mathbf{r})} \tag{2.8}$$

Inserting this effective potential in equation (2.5) the wave functions for the problem can be found with the same methods as in the case of non-interacting electrons. This offers a great simplification of the problem since it is straight-forward to solve the problem for non-interacting electrons.

If the exact exchange-correlation functional were to be used, the method above would give the exact wave functions and all the properties of the molecule could be determined exactly. Unfortunately, there is no known exact exchange-correlation functional and this introduces an error to the solution. Major work has been devoted to finding the exchange-correlation functional that gives the best description and there are today an abundance of suggested energy functionals [16]. Different functionals typically works well in different situations and which functional to use for a particular problem is the trick of the trade of DFT. The functional called B3LYP is the most widely used in the literature and according to Sousa *et al* [16] it has been used in 80 % of the published DFT studies between 1990 and 2006. The significant impact of DFT methods on the scientific community was the reason why W. Kohn was awarded the Nobel Prize in Chemistry in 1998.

Chapter 3

Charge transport in organic materials

To understand the behavior of electronic devices, an in-depth understanding of how electrical charges travel through the material is required, as well as how these are affected by external parameters such as the applied voltage. In general, electrical current can be carried by both electrons and ions. However, in solid-state materials the electronic currents dominate over ionic currents, due to the higher mobility of electrons as compared to the bulkier ions. In this chapter a brief overview of the electronic charge transport processes of organic materials is given.

In crystalline inorganic semiconductors the atoms are perfectly aligned in a lattice, allowing for good orbital overlap between neighboring atoms and an associated delocalization of the electronic states throughout the material [19, 20]. In such materials charges are transported by band-like motion and the mobility is very high. Any deviation in the lattice (impurities, dislocations etc) results in a perturbation of the delocalized states and as a consequence the mobility decreases. In the extreme case of many imperfections (as the case with amorphous semiconductors) the electronic states becomes localized over a small volume. The limiting factor for charge transport is then hopping between such localized states.

In organic materials, on the contrary, disorder is the rule rather than the exception, partly due to the simple and cheap processing methods commonly employed and partly due to the more complicated geometry and composition of the molecules. Furthermore, adjacent molecules couples to each other via weak Van der Waals interactions with little orbital overlap. Consequently the probability for transfer of carriers between them is low. Therefore, charge carriers are in general transported via hopping between sites with randomly

varying energy levels and inter-site distances, see figure 3.1. The energetic- and spatial disorders are sometimes referred to as diagonal- and off-diagonal disorder, respectively. For low electric fields the spatial disorder is believed to be the origin of the negative field dependence on the mobility commonly observed [21].

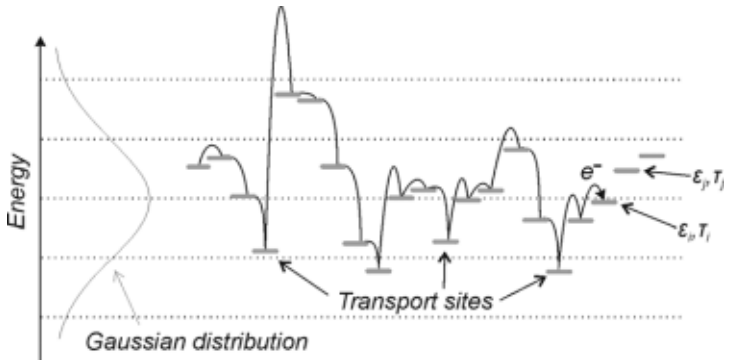

Figure 3.1: Electron hopping within Gaussian distribution (width σ) of transport states. Each state is defined by an energy, ε_i, and the width of the distribution is σ. Depending on the energy difference to the next site (i.e. $\varepsilon_i - \varepsilon_j$) the electron will reside on the site for a time τ_i.

3.1 Disorder in organic materials

The energetic disorder in organic solids originates from the random orientation of the dipole moments of polar molecules or of the quadrupole moment of non-polar molecules [22-25], see figure 3.2. It is straightforward to determine the distribution in the case of polar molecules. Assume that a fraction c of the molecules have a dipole moment and that this dipole moment is randomly oriented in such case. The electrostatic energy of site i, ε_i, due to the surrounding dipoles is then given by:

$$\varepsilon_i = -\frac{q}{4\pi\varepsilon_0\varepsilon_r}\sum_n \frac{\mathbf{r}_{in}\cdot\mathbf{p}_n}{r_{in}^3} \qquad (3.1)$$

where $\mathbf{r}_{in}$ is the vector from site i to site n and $\mathbf{p}_n$ is the dipole moment of site n. Given a large set of sites the distribution of ε_i's converges towards a Gaussian distribution, given by [22]:

$$g(\varepsilon) = \frac{1}{\sqrt{2\pi}\sigma} \exp\left(-\frac{\varepsilon^2}{2\sigma^2}\right) \tag{3.2}$$

where the magnitude of the disorder is defined by σ. It can be shown that for a simple cubic lattice (i.e. ignoring spatial disorder) with random dipoles σ is given by [26]:

$$\sigma = \frac{2.35qp}{4\pi\varepsilon_0\varepsilon_r a^2} \tag{3.3}$$

where p is the dipole moment of the molecule and a is the lattice constant. Typically, σ is near 0.1 eV in organic solids.

The electrostatic potential due to dipoles extends over long-ranges (~1/r). Therefore, the electrostatic environment of two neighboring sites is not likely to differ completely. To achieve a fully accurate description of the disorder this interaction has to be taking into consideration [27, 28]. The correlation function for neighboring sites with dipolar energies defined by (3.1) has been derived by Gartstein *et al* [27]:

$$f_{ij} = \left\langle \varepsilon_i \varepsilon_j \right\rangle = \frac{q^2}{(4\pi\varepsilon_0\varepsilon_r)^2} \sum_n \frac{\mathbf{r}_{in} \cdot \mathbf{r}_{jn}}{(r_{in} r_{jn})^3} \left\langle \mathbf{p}_n^2 \right\rangle = \frac{q^2}{(4\pi\varepsilon_0\varepsilon_r)^2} \frac{cp^2}{3} \sum_n \frac{\mathbf{r}_{in} \cdot \mathbf{r}_{jn}}{(r_{in} r_{jn})^3} \tag{3.4}$$

It is hard to find a closed form expression for the correlated Gaussian distribution and most studies rely on Monte Carlo simulations. While the energy levels within a Gaussian distribution might vary a lot from site to site, the correlated disorder distribution rather forces the energy levels to fluctuate over larger distances.

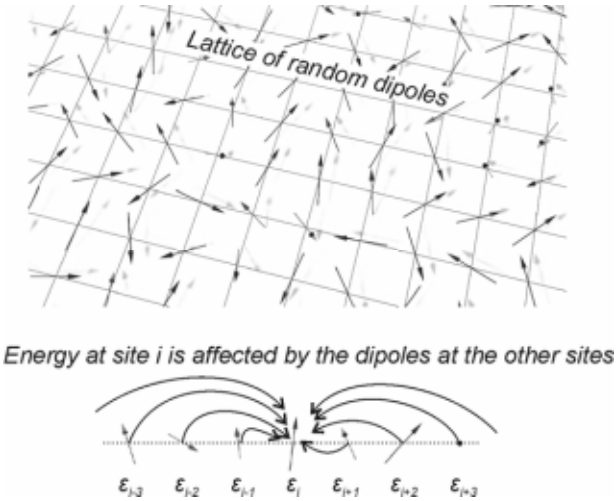

Figure 3.2: The energetic disorder is due to the random orientation of the molecules and consequently also the random orientation of their dipoles or quadrupoles. The energy of site ε_i is the sum of the contribution of the electrostatic interaction with the surrounding molecules.

The interface between organic materials and electrodes are usually not very clear-cut, due to diffusion of metal species and chemical reactions during deposition as well as the intrinsic softness and roughness of the organic surface. Therefore the disorder near the interface is most likely considerably different from that in the bulk. Intuitively one might argue that disorder should increase toward the interface. However, Novikov *et al* [24] showed by theoretical calculations that disorder at the interface is suppressed since the metallic electrode is an equipotential surface. The disorder parameter, σ_0, as a function of distance from the interface, z, is given by:

$$\sigma_0^2(z) \approx \sigma_b^2\left(1-\frac{a_0}{2z}\left(1-\exp\left(-\frac{2z}{a_0}\right)\right)\right), \qquad a_0 = 0.76a \tag{3.5}$$

where a is the lattice constant and σ_b is the disorder in the bulk given by:

$$\sigma_b^2 = \frac{4\pi e^2 p^2 c}{3\varepsilon_0^2 \varepsilon_r^2 a^3 a_0} \tag{3.6}$$

where p is the dipole moment of a molecule in the organic media and c is the fraction of sites occupied by dipoles. It has also been shown that roughness at the interface could not contribute to a significant increase in disorder (σ_r ~10 meV) [29].

3.2 Models for charge transport in organic materials

From a microscopic point of view charge transport involves the transfer of charge from one molecule (A) to another (B). This can be regarded as a redox reaction with the reduction (oxidation) of the starting molecule and the oxidation (reduction) of the final molecule in the case of a positive (negative) polaron, see figure 3.3. Repeating the charge transfer process many times can simulate the motion of a charge carrier and disorder can be introduced by randomizing the exact position and rotation of the molecules.

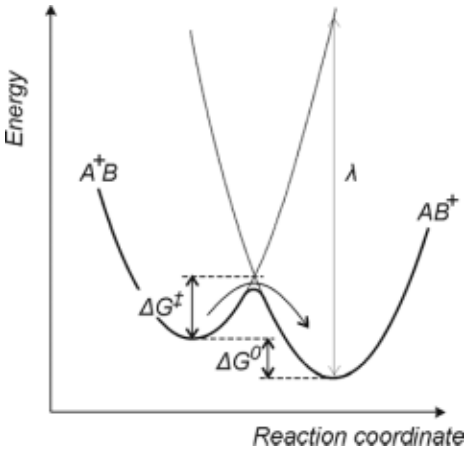

Figure 3.3: Charge transport involves the transfer of charges between two adjacent molecules, A and B. A^+B and AB^+ denote the combined system of the two molecules where only molecule A or only molecule B is charged. ΔG^0 is the Gibbs free energy of the reaction, $\Delta G^‡$ is the barrier for the reaction and λ is the reorganization energy.

The jump rate of the charge carriers from molecule A to molecule B, or equivalently the reaction rate is given by Marcus theory [30, 31]:

$$v_{Marcus} = \frac{2\pi}{\hbar}\left|V_{if}\right|^2 \sqrt{\frac{1}{4\pi\lambda k_B T}} \exp\left(\frac{-\left(\Delta G^0 + \lambda\right)^2}{4\lambda k_B T}\right) \tag{3.7}$$

where V_{if} is the electronic coupling matrix element for transition between state i and j and ΔG^0 is the change in Gibbs free energy due to the charge transfer. λ is the reorganization energy and is related to the polaron binding energy. While this can give insight into the microscopic transfer process it becomes a cumbersome technique for investigation of practical system, constituting a large set of molecules.

The pioneering work of Bässler [21] forms the ground work for the last decades rapid progress in the understanding of charge transport in organic electronic devices. His model disregards the exact chemical nature of the molecules. Instead, the transport sites are described by a Gaussian distribution of energy levels and inter-site distances. The model neglects the effect of polarons, assuming that σ of the site distribution is larger than the polaron binding energy. Consequently the somewhat simpler Miller-Abrahams jump rate, v_{MA}, is used:

$$\begin{aligned} v_{MA} &= v_0 \exp\left(-2\gamma R_{ij}\right) \cdot \begin{cases} \exp\left(-\dfrac{\varepsilon_j - \varepsilon_i}{k_B T}\right), & \varepsilon_j > \varepsilon_i \\ 1, & \varepsilon_j < \varepsilon_i \end{cases} = \\ &= v_0 \underbrace{\exp\left(-2\gamma R_{ij}\right)}_{Spatial} \underbrace{\mathrm{Bol}\left(\varepsilon_j - \varepsilon_i\right)}_{Energetic} \end{aligned} \tag{3.8}$$

where the carrier hops from site i to j. R_{ij} is the distance between site i and j, γ is connected to the spatial overlap of the states i and j, and ε_i and ε_j is the energy of site i and j. In other words hopping downwards in energy has unit probability, while the probability for hopping upward in energy decreases exponentially with

energy. Novikov al [28] found that the mobility of the charge carriers in a system described by the Bässler model and a correlated Gaussian disorder (e.q. 3.2) is given by:

$$\mu = \mu_0 \exp\left(-\left(\frac{3\sigma}{5k_B T} \right)^2 + C_0 \left(\left(\frac{\sigma}{k_B T} \right)^{3/2} - \Gamma \right) \sqrt{\frac{eaE}{\sigma}} \right) \tag{3.9}$$

where σ and Γ is the width of the energetic and spatial Gaussian distribution respectively and C_0 is a constant determined from simulations. In [28] C_0 and Γ is set to 0.78 and 2 respectively. Even though this so-called correlated disorder model (CDM) originally was developed for transport of charge carriers in molecularly doped polymers, relation (3.9) describes the mobility of charge transport in conjugated polymers remarkably well over a wide range of electric field.

A limitation of the correlated Gaussian disorder model is that it does not include any dependence on the carrier concentration, p. However, the carrier concentration has to be taken into consideration in order to explain the much higher mobility measured in transistors as compared to the mobility measured in diodes for the same material. In transistors the carrier concentration can exceed 0.1 carriers per site, while in diodes the carrier concentration is typically much smaller, in the range of 10^{-6}-10^{-3} carriers per site. The carrier concentration dependence on the mobility can be understood by considering the occupied density of states (ODOS) as the carrier concentration is increased, see figure 3.4.

It can be assumed that the majority of the carriers that contributes to the transport reside in states near the maximum of the ODOS (ε_{max}, illustrated as circles in figure 3.4). At higher energy there are more empty states available to jump to. On the other hand, it is clear from equation (3.8) that the probability for hopping decreases as the energy difference between initial and final states, Δε, is increased. Taking both these arguments into consideration it is possible to find an optimal transport energy, ε_t, to which the transition rate from ε_{max} is maximized [32]. Furthermore, it turns out that ε_t is effectively independent on the carrier concentration. In other words, with these assumptions the carrier

transport is limited by jumps from ε_{max} to ε_t. At low p the carriers occupy states deep down within the tail of the DOS and ε_{max} is constant with respect to p. Consequently, $\Delta\varepsilon$ is approximately constant, resulting in a mobility that is independent on the carrier concentration. As p is increased above a certain limit (corresponding to E_F > -0.5 eV in figure 3.4) ε_{max} starts to shifts towards higher energy, resulting in a reduction of $\Delta\varepsilon$ and an associated increased mobility.

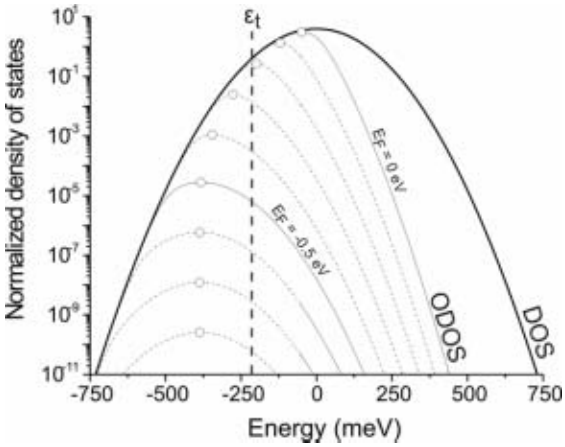

Figure 3.4: The shape of a Gaussian density of states (DOS) with σ = 100 meV and the occupied density of states (ODOS) for several values of the Fermi level (E_F). The circles mark the maximum of the ODOS.

Recently, several investigators have presented models describing the charge carrier mobility in organics solids incorporating the dependence of carrier concentration [33, 34]. Pasveer *et al* [34] has presented a model of the mobility that is both field- and charge carrier concentration dependent. According to this model, that has also been experimentally verified with great success, the carrier concentration dependence is dominating at room temperature when the field is not very high. At low temperature or at high field the electric field dependence becomes important.

The Pasveer mobility is given by:

$$\mu(T, p, E) = \mu_p(T, p)\mu_E(T, E) \tag{3.10a}$$

where

$$\mu_p(T, p) = \mu_0 \exp\left(-0.42\left(\frac{\sigma}{k_B T} \right)^2 + \frac{1}{2}\left(\left(\frac{\sigma}{k_B T} \right)^2 - \frac{\sigma}{k_B T} \right)\left(2pa^3 \right)^\delta \right) \tag{3.10b}$$

and

$$\mu_E(T, E) = \exp\left(0.44\left(\left(\frac{\sigma}{k_B T} \right)^{3/2} - 2.2 \right)\left(\sqrt{1 + 0.8\left(\frac{Eea}{\sigma} \right)^2} - 1 \right) \right) \tag{3.10c}$$

The exponent δ in (3.10b) is given by

$$\delta = 2\frac{\ln\left((\sigma/k_B T)^2 - \sigma/k_B T \right) - \ln(\ln 4)}{(\sigma/k_B T)^2} \tag{3.10d}$$

Note that the carrier concentration becomes more important as the disorder in the material is increased.

3.3 Charge transport related to devices

Two terminal devices, such as light emitting diodes and photovoltaic devices, are in general built up in a vertical geometry with the active material sandwiched between two conducting electrodes, see figure 5.2 in chapter 5. Depending on the rate limiting process, the current through the active material can be classified as either charge injection limited or space charge limited. In the case of injection-limited current (ILC), the charge transport through the device is

limited by the injection of charge carriers from the metal electrode into the bulk of the organic material. Once charges are injected they can easily move through the bulk of the device. In the case of space charge limited current (SCLC), the rate of injection of charges is higher than the rate at which the charge carriers are transported away from the interface region, resulting in a build up of space charge. This will cause an opposed field that suppresses further injection of charges and hence the current is limited by at what rate carriers can be transported through the bulk of the material.

Upon investigating the charge transport properties of devices one must first determine whether the current is limited by injection processes or by bulk transport [35, 36]. One straightforward way to do this is to study how the current level, at a specific voltage to thickness ratio, changes upon varying the thickness of the organic layer of the devices. In the case of ILC there is no such thickness dependence of the current. Although it might be tempting to interpret the often exponentially growing current for small voltages in diodes as ILC, it is imperative to stress that this is not always the case. Since the mobility in organic materials tend to be dependent on the electric field, exponentially growing current can very well also be observed in devices with purely SCLC transport processes [37, 38].

The two electrodes of an organic device are often made of two different materials with different work functions, resulting in a built-in potential across the device. In order to make a correct assessment of the charge transport properties this built in potential must be compensated for. If this is not done wrong conclusions about the transport behavior can be drawn [37]. To a first approximation the built-in potential could be described as the difference in work function between the electrodes. However, it is sometimes difficult to tell the exact values of the work function since the interface between the organic material and the electrodes are usually not well defined. Chemical reactions between the metal electrode and organic material might cause a change in work function. In addition, dipoles at the interfaces increase or reduce the actual difference of the work function depending on their orientation. Therefore it is

important to directly measure the built-in potential before assessing the charge transport properties of a device.

An simple way to determine the built-in potential is by photovoltaic measurements [39-41]. When the sample is illuminated with photons of an energy greater than the optical band gap of the material charge carriers will be excited across the band gap. In the absence of an applied voltage these charge carriers will migrate in the field entirely caused by the built-in potential, resulting in a photocurrent. The built-in potential can be estimated simply by measuring at what voltage the photocurrent vanishes as the externally applied voltage is varied. To get an accurate result, diffusion of thermally excited charge carriers need to be accounted for. In other words the correct built-in potential is found when the net photocurrent, i.e. the current under illumination minus the dark current, is zero.

3.3.1 Injection limited current

Traditionally charge injection from a metallic contact into an ordered material has been treated with either the Fowler-Nordheim (FN) or the Richardson-Schottky (RS) formalism [20]. FN describes tunneling injection of the charges through a triangular potential barrier, caused by the tilt of the energy band, and is given by:

$$j(F) = BF^2 \exp\left[-\frac{4\left(2m_{eff}\right)^{1/2} \cdot \Delta^{3/2}}{3\hbar eE}\right] \tag{3.11}$$

The abundance of charge carriers in the metal will rearrange to screen any electric field, so that the electric potential inside the metal is always constant. A charge in the organic material will therefore experience an electric field due to the rearranged charges in the electrode. This is the so-called image charge that will cause a strong energy band bending at the interface. If the injected charge carrier does not escape the image charge potential it will be extracted back to the

metal, thus not contributing to the injection current. Richardson-Schottky thermionic emission treats charge carriers thermally excited above the barrier for injection including image charge:

$$j(F) = CT^2 \exp\left[-\left(\Delta - \left(\frac{eE}{4\pi\varepsilon\varepsilon_0} \right)^{1/2} \right) \Big/ kT \right] \tag{3.12}$$

The fundamental problem with both FN and RS when dealing with organic materials is that they were developed for charge injection into ordered materials with delocalized states and hence true band transport. As have been shown above this is in general not the case in organic materials, where disorder prevails. Even though the FN and RS models could be used in some cases to verify experimental data, they do not explain any of the physics behind the processes.

Several models for charge injection into disordered materials have been developed [42-44]. Pioneering this evolution was the work by Arkhipov *et al* [42, 45, 46]. Their model assumes that the first jump from the metal electrode into the organic solid is the "hardest" and hence the rate limiting process. Therefore only the first jump is taken into consideration. Assume that all charge carriers start at the Fermi level of the metal and that this level is the reference level and set to zero. Assuming that the Miller-Abrams formalism is appropriate, then the jump rate for such carriers injected into a state a distance x from the electrode and at an energy of E is given by:

$$\nu_{MA} = \nu_0 \exp(-2\gamma x)\mathrm{Bol}(E) \tag{3.13}$$

To determine the total jump rate of charge carriers into the organic material (3.13) is integrated over the distance of the organic layer and over all available energy levels. The spatial integration is from the first jump site, at a distance a from the electrode, towards infinity. In reality the upper limit is the distance to the next electrode. However since the probability for jumps decreases exponentially with distance it can be approximated to infinity with very little

error. Allowed energy levels are given by the Gaussian distribution, g(E), centered around the mean energy, U(x), given by:

$$U_0(x) = \Delta - eEx \tag{3.14}$$

where Δ is the difference between the LUMO (HOMO) and the metal work function for injection of electrodes (holes), and eEx is energy contribution of the applied electric field.

With this, the injection current is given by:

$$j_{inj} = ev_0 \int_a^{\infty} \int_{-\infty}^{\infty} \underbrace{\exp(-2\gamma x)}_{Spatial} \underbrace{\mathrm{Bol}(E) g[U_0(x) - E]}_{Energetic} dE\, dx \tag{3.15}$$

In order to take image charges into consideration the spatial part of equation (3.15) need to be modified. The probability for a charge carrier, injected to a site at a distance x from the interface, to escape from its image charge is denoted $w_{\mathrm{esc}}(x)$. Only those charges that do escape from their image charge will contribute to the current, since the others are extracted back to the electrode again. It turns out that w_{esc} can be described by the Onsager equation for the yield of photo generation in one dimension [47, 48], given by:

$$w_{esc}(x) = \frac{\int_a^x ds \exp\left(-\frac{e}{kT}\left(Es + \frac{e}{16\pi\varepsilon_0\varepsilon_r s}\right)\right)}{\int_a^{\infty} ds \exp\left(-\frac{e}{kT}\left(Es + \frac{e}{16\pi\varepsilon_0\varepsilon_r s}\right)\right)} \tag{3.16}$$

Furthermore, the mean site energy needs to be modified to include the image charge potential according to:

$$U(x) = \Delta - \frac{e^2}{16\pi\varepsilon_0\varepsilon_r x} - eF_0 x \tag{3.17}$$

Together this gives the total injection current including image charge effects:

$$j_{inj} = ev_0 \int_a^{\infty} \int_{-\infty}^{\infty} \underbrace{\exp(-2\gamma x) w_{esc}(x)}_{Spatial} \underbrace{\mathrm{Bol}(E) g[U(x) - E]}_{Energetic} dE\, dx \tag{3.18}$$

In figure 3.5 the injection current according to (3.18) is plotted for several values of the injection barrier, Δ, and disorder width, σ. It turns out that while disorder limits bulk transport, it can improve charge injection. This is qualitatively illustrated in figure 3.6 where the transport levels (band edge) in a perfectly ordered material are compared to the levels in a disordered material. The disorder introduces allowed states lower in energy that in the ordered case, hence reducing the barrier for injection.

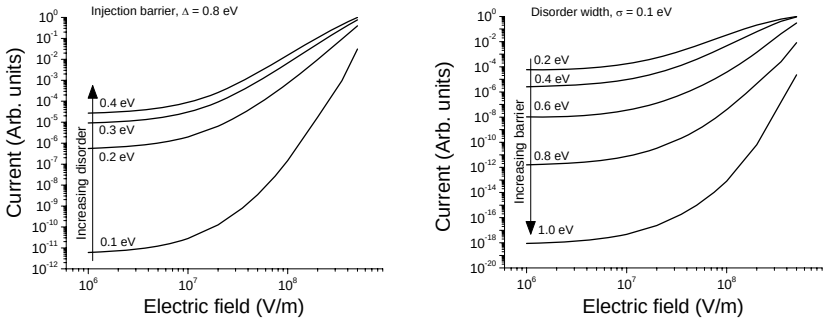

Figure 3.5: Injection current according to the Arkhipov model, given by equation (3.18). The current is parametric in barrier height, Δ, and disorder width, σ, to the left and right respectively

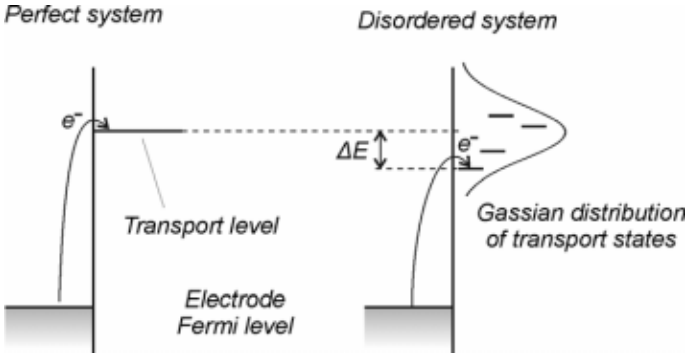

Figure 3.6: Qualitative illustration of the improved electron injection for a disordered system.

In order to improve charge injection, reduction of the barrier height Δ is desired. One way to do this is to modify the work function of the electrode, for example by introducing a dipole layer on top of the electrode [49-52]. In paper 2 of this thesis, adsorption of the strong donor tetrakis-(dimethylamino)ethylene (TDAE) onto a PEDOT:PSS surface is reported. Electrons are transferred from TDAE to PEDOT chains, reducing the surface PEDOT layer and positively charging the TDAE molecule. In this way a dipole is formed at the surface, resulting in lowering of the PEDOT work function from 4.8eV to 3.9eV.

3.3.2 Space charge limited current

If the charge injection rate is higher than the rate of transport through the material the current is space charge limited (SCLC). In the case of a constant mobility the SCLC current is given by Childs law [9]:

$$J_{Child} = \frac{9}{8}\varepsilon_0\varepsilon_r\mu\frac{V^2}{d^3} \tag{3.19}$$

However, as have been discussed above, the mobility in organic disordered systems are not constant but dependent on both the electric field and the charge carrier concentration in the device. Unfortunately, it is non-trivial to find an analytical expression for the current density versus voltage in the case of an electric field- and carrier concentration dependent mobility, since the field and the charge concentration is not homogenous throughout the material. However, the current density can be found numerically by solving a system of differential equations.

Assume the current is carried by only one type of charge carriers (i.e. holes or electrons only) and that the device consists of only one layer sandwiched in between two metal electrodes. If diffusion is neglected the current density, J, is given by:

$$J = q\rho(x)\mu(E(x),\rho(x))E(x) \tag{3.20}$$

where q is the charge of the carrier, i.e. –e or e for electrons and holes respectively. ρ(x) is the charge carrier concentration, μ is the electric field- and carrier concentration dependent mobility given by (3.9) or (3.10) and E(x) is the electric field. In steady-state the current density must be constant with respect to the position in the device. Using (3.20) this gives:

$$\frac{dJ}{dx} = 0 \quad \Rightarrow \quad \frac{dp}{dx} = -\frac{e}{\varepsilon_0 \varepsilon_r} \frac{\left((du/dE)E + u\right)p^2}{\left((du/dp)p + u\right)E}$$

The charge carrier concentration, ρ(x), is given by Poisson's equation:

$$\frac{d^2\Psi(x)}{dx^2} = -\frac{q}{\varepsilon_0 \varepsilon_r}\rho(x) \tag{3.21}$$

where Ψ(x) is the electrical potential given by E = – dΨ(x)/dx. The problem of calculating the current-density in the device can then be summarized as a system of non-linear ordinary differential equations given by:

$$\begin{cases} \dfrac{d\rho}{dx} = -\dfrac{e}{\varepsilon_0 \varepsilon_r} \dfrac{\left((du/dE)E + u\right)p^2}{\left((du/dp)p + u\right)E} \\ \dfrac{dE}{dx} = \dfrac{q}{\varepsilon_0 \varepsilon_r}\rho \\ \dfrac{d\Psi}{dx} = -E \end{cases} \tag{3.22}$$

With three unknown variables (ρ, E and Ψ), three boundary conditions are required in order to solve the system of differential equations. Two boundary conditions are the electric potential at the two contacts. For simplicity it can be assumed that the voltage is applied to the injecting contact (*i.e.* x=0) while the extracting contact (*i.e.* x=t) is grounded, i.e. $\Psi(0) = V_{Appl}$ and $\Psi(t) = 0$. The carrier concentration at the injecting contact can be used as the last boundary condition, i.e. $\rho(0) = \rho_0$. This can be regarded as a measure of how easily charge carriers are injected into the organic material. If ρ_0 is low the current density will be limited by charge-injection from the contacts. Since this discussion regards SCLC, ρ_0 then must be set to a value that is high enough to not affect the solution of the system of differential equations. A value of $\rho_0 = 10^{25}$ m^{-3} satisfies this requirement and can therefore be used.

In figure 3.7 the resulting current density is shown for the case of correlated Gaussian disorder mobility (equation 3.9), the Pasveer mobility (equation 3.10) as wells as the case of a constant mobility. The field- and/or carrier concentration dependence result in a significantly higher current at high fields as compared to the case of a constant mobility. Also shown in figure 3.7 is the charge carrier- and electric field distribution in the material. As expected, there is a high concentration of charges near the injecting contact, resulting in a vanishing electric field. By curve-fitting experimental data for a range of temperatures to the calculated J-V behavior material parameters such as width of disorder and average intersite distance can be assessed [53] .

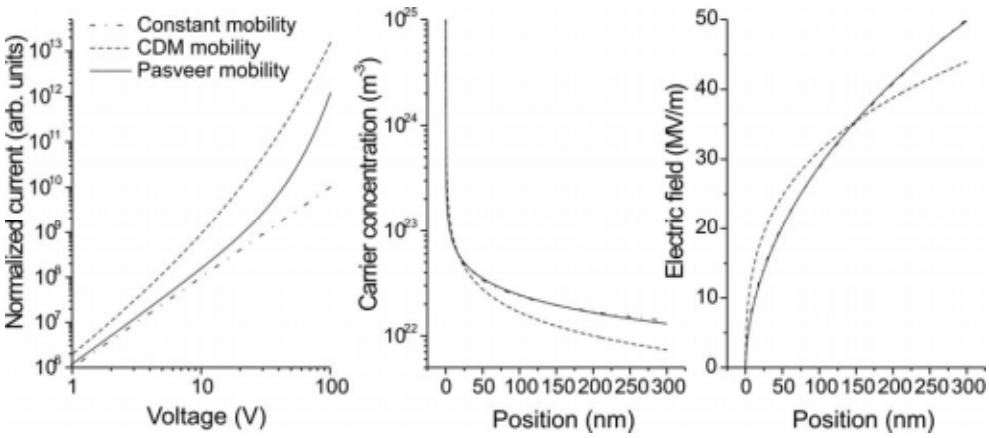

Figure 3.7: To the left the space charge limited current with constant mobility, CDM mobility and Pasveer mobility is shown. In the middle and to the right the charge carrier concentration and electric field across the device is shown at an applied voltage of 10V. In all cases the temperature is 295 K, the device thickness is 300 nm, σ = 100 meV and the average intersite distance a = 1 nm.

Chapter 4

Resistance switching in organic materials

As described in chapter 3 several parameters, such as charge carrier concentration or mobility, affect charge transport in organic materials. By controlling any of those parameters, the conductivity can be modulated, something that potentially can be very useful for electronic devices. Modulation of charge transport can be achieved by stressing the material with some external stimuli, such as light, heat, pressure or electric field. This is for example used in transistors where the charge carrier concentration is modulated as a function of an electric field, resulting in a dramatic change of conductivity. However, when the electric field is removed the carrier concentration returns to the original level again. In some materials the charge transport properties can be switched stably between two states upon exposure to external stimuli, i.e. the material remains in the state even after the external stimuli is lifted. These bistable switch materials can be used in electronic devices such as in sensors and memories.

In a sense the electrical conductivity of any material can be switched in an irreversible fashion as the intensity of the applied stimuli exceeds a certain threshold value. For example, if the current becomes too large through the material it can undergo a rapid and destructive reaction due to the dissipated heat. The effect is a catastrophic breakdown causing an irreversible and dramatic change of the charge transport properties. Organic devices based on such breakdown mechanism have been suggested and explored for so-called write once read many (WORM) devices [54].

Followed is a brief review of some of the reversible switch mechanisms that have been suggested for devices based on organic materials. A excellent review can be found in ref [55].

4.1 Switching of molecular configuration and conformational changes

Some molecules have more than one stable configuration, with different orbital spatial distribution and associated energy levels [4, 56]. The π-orbital overlap within the molecule or between adjacent molecules could be significantly different in the different states, resulting in a difference in mobility. Such a system can be described by the illustration in figure 4.1, where the states A and B are separated by an energy barrier, ΔE, and at energy levels E_A and E_B, respectively. Upon exposing the molecule to some external stimuli the molecule can be excited above ΔE and change its state. In theory the system will return to the lowest energy state given enough time. However, if ΔE is sufficient this will take a very long time and both states appears to be stable.

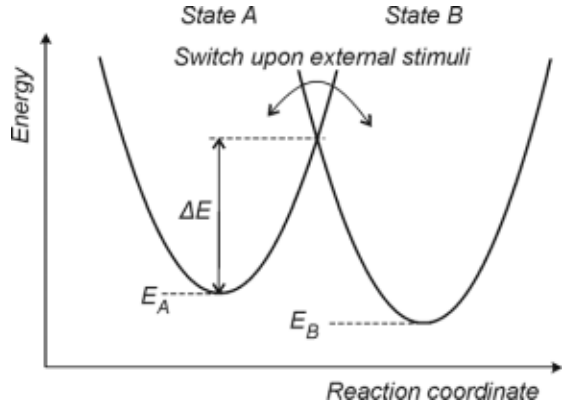

Figure 4.1: Illustration of the energy levels of the two (quasi) stable states. If the external stimuli supply sufficient energy (>ΔE), the system can change state.

If the HOMO or LUMO levels are different in the two states this will have an impact on the transport properties of the material. At the interface, switching of the energy levels will alter the barrier for injection of holes or electrons (top left in figure 4.2). If a bistable molecule is blended into a host material, a change

in energy levels can result in the appearance of states within the HOMO – LUMO gap of the host material. At the interface, these states might act as intermediate states, providing injection paths via several smaller hops rather than one big hop. Since the former is more favorable than the latter this can greatly improve charge injection. In the bulk, the gap states can instead act as traps resulting in reduced mobility (top right in figure 4.2). Hence, charge injection and bulk transport are two competing processes. An example of a photochromic molecule with switchable HOMO and LUMO levels is shown in the bottom of figure 4.2. The concept of switchable charge traps and injection barrier have been demonstrated by Andersson *et al* [57] and Tsujioka *et al* [58] respectively.

As the molecule change conformation it is possible that its dipole moment is also changed. This will change the width of the distribution of the transport states, σ, as is evident from chapter 3. An increased σ results in better charge injection, but also worse bulk charge transport, analogous to the case of switchable gap states. Note that in this case the transport site distribution is still centered on the same energy level. Moreover, the average energy barrier for hopping to adjacent sites is still considerably lower than that envisaged for switchable gap states. Another effect of dipoles at the interface was described in chapter 3: if the dipole moments of the molecules can be switched the barrier for injection, i.e. the energy difference between metal work function and HOMO or LUMO levels, will also change.

If only a part of the molecules change dipole moment a third effect can be envisaged: switchable dipole traps. This can for example be achieved by blending guest molecules with switchable dipole moment into a host matrix. As the dipole moment of the guest molecules is changed the electrostatic landscape in the vicinity of those molecules is changed. Depending on the position of the neighboring states with respect to molecular dipole orientation some states will acquire a higher energy and others a lower energy. The states with lower energy will then act as traps for charge carriers. In this way, a molecule with a switchable dipole moment can induce traps even though its HOMO/LUMO levels

are the same as the host material. Nešpůrek *et al* [59, 60] have studied the effect of such switchable dipole moments.

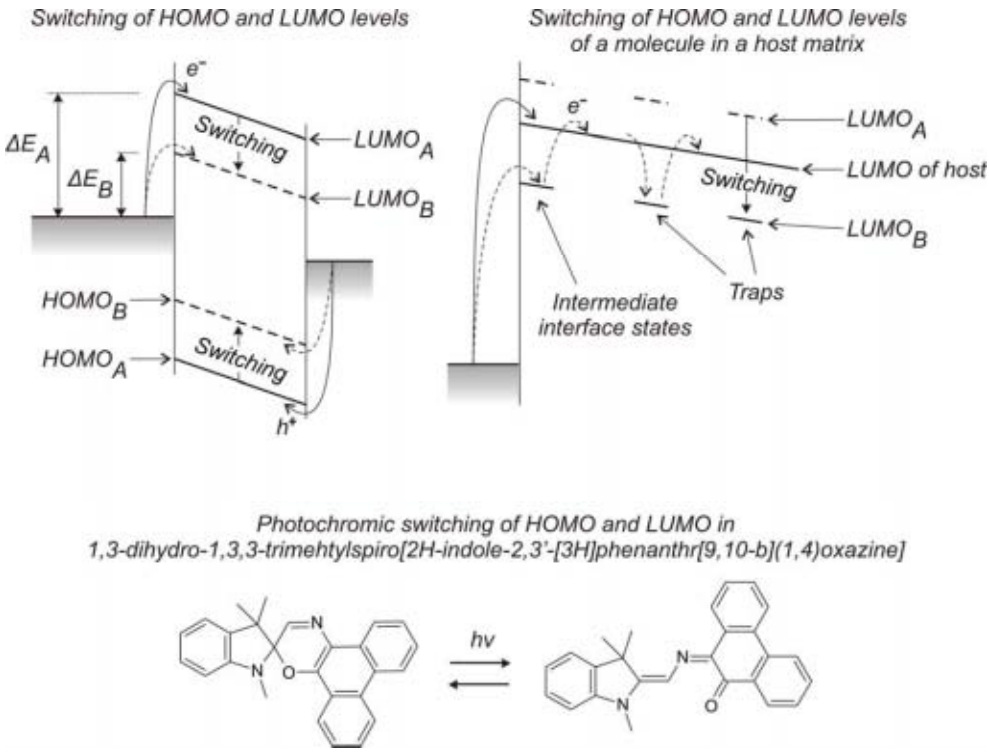

Figure 4.2: The injection barrier can be switched if the HOMO and LUMO level can be switched (top left). If a molecule with switchable HOMO and/or LUMO is blended into a host material, switchable charge traps can also be achieved (top right). In the bottom of the figure is an example of a photochromic molecule with switchable HOMO/LUMO levels shown.

The change in orbital configuration might lead to a geometrical conformational change of the molecule, such as rotations around a bond. This might lead to an alignment of the π-orbital overlap between different parts of the molecules, resulting in a more conjugated system. As a consequence the mobility along the molecule is increased. This has been suggested to be the case for Rose Bengal, where the neutral molecule is twisted while the charged molecule is

planar (see figure 4.3) [61]. In the twisted conformation the overlap between orbitals is poor between the perpendicular segments. However, as the molecule becomes planar the orbitals line up in the same plane and hence the overlap is significantly improved. A conformational change might also lead to a change of the packing efficiency of the molecules and hence a change in the π-orbital overlap between adjacent molecules.

It might be hard to get a clear-cut case were only one of the above mentioned effects take place. Several of these effects are interlinked and will most likely coexist.

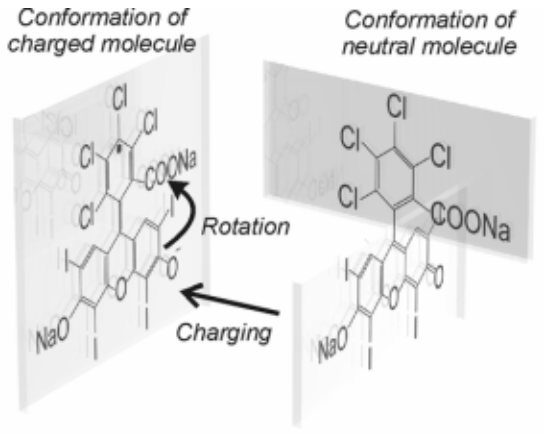

Figure 4.3: When the Rose Bengal molecule is charged it changes conformation and becomes planar, thus improving conjugation along the molecule.

4.2 Charge transfer salts

Charge transfer complexes are materials consisting of a donor-acceptor pair, either internally within a molecule or by the combination of two species with low ionization potential and high electron affinity, respectively. These materials have been studied extensively for several decades due to their interesting electrical properties [62-64]. In charge transfer materials the molecules are charged due to

transfer of electrons from the donor- to the acceptor species. Strong effects can be found in charge transfer materials were the molecules are well ordered and act collectively. In such systems the donors (D) and acceptors (A) either stacks in separate stacks or alternates within the same stack [9, 65], see figure 4.4.

The energy cost of transferring an electron from a donor to an acceptor is equal to the cost to ionize the donor, i.e. the donor ionization energy I_D, minus the energy gained by ionizing the acceptor, i.e. the electron affinity A_A. On the other hand, the system gains in electrostatic energy to become ionized due to the attractive interaction between the oppositely charged ions, expressed by the Madelung energy, E_M. The Madelung energy is the energy gained due to interionic Coulombic interaction by the system when the donors and acceptors are ionized.

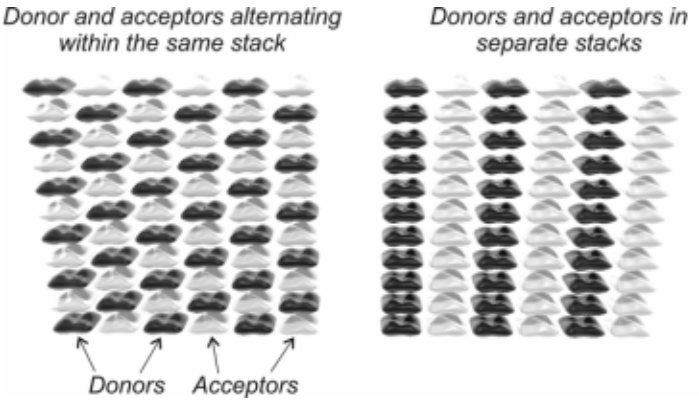

Figure 4.4: Separate stacks of donor and acceptor molecules (right) or alternation of donor and acceptor within the same stack (left).

Hence the net energy difference per molecular site of the system, E_B^F upon ionization is given by [65]:

$$E_B^F = (I_D - A_A) - E_M \tag{4.1}$$

If $E_B^F > 0$ the energy gained by the ionization is less than the cost and the state is unstable. In this case partial charge transfer is favored as long as the net energy per molecule, $E_B(\rho)$ is lowered [64]:

$$E_B(\rho) = \rho(I_g - A_g) - E_M(\rho) \tag{4.2}$$

where ρ ($0 \leq \rho \leq 1$) is the degree of charge transfer. Partial charge transfer should in this case mean that the molecules are only partially ionized. Stacks with complete or no charge transfer ($\rho = 0$ or $\rho = 1$) has filled energy bands and hence acts as insulators or semiconductors, depending on the width of the band gap. For partial charge transfer however the outer band is only partly filled, resulting in metallic conduction. Note that to get truly metallic conduction the inter-molecular distance must be constant throughout the stack. A periodicity in distance leads to semiconducting behavior due to Peierl's distortion [9]. The structure with separate stacks of donors and acceptors results in anisotropic conductivity with high conductivity along the stacking direction and much lower conductivity in the direction perpendicular to the stacking direction (one-dimensional metals).

In some materials the site energy is similar for the neutral and ionized states and in that case both states are stable. This opens up the possibility to switch between the neutral insulator state and the ionized highly conducting state upon exposure to some external stimuli. Such switching have been suggested to be the origin of resistance switching using pressure stimuli [64], electrical stimuli [63, 66] and optical stimuli [67]. Schematic transition scheme upon stimuli is given by:

$$[D^+A^-]_n \leftrightarrow [D^0A^0]_x + [D^+A^-]_{n-x} \tag{4.3}$$

In other words some molecules are neutralized resulting in an overall partial charge transfer, which leads to unfilled bands and high conductivity. Typical charge transfer salts are the acceptor tetracyanoquinodimethane (TCNQ) complexed with Cu or Ag (Cu-TCNQ and Ag-TCNQ) or with organic donor

molecules such as tetrathiafulvalinium (TTF-TCNQ). Cu-TCNQ have be extensively studied as potential candidate for memory applications [68].

4.3 Metal cluster switching

Conductance switching has been observed in systems with metal clusters blended into an insulating or semiconducting matrix. This effect was first observed several decades ago in inorganic materials and was explained by Simmons *et al* [69]. In organic materials the effect was first reported by Ma *et al* [70-73], and later by Bozano *et al* [74] who studied metal cluster switching in a wide range of systems combining nano particles with both spin cast polymers and also with evaporated small molecules. The group of Österbacka have reported similar switching behavior in an all-organic device based on C_{60} in a polystyrene matrix [75, 76].

According to Simmons the metal clusters (or C_{60}) act as transport states in the band gap of the insulating matrix. In the ON state charges are transported by hopping through these states. If the applied voltage is removed quickly charge is trapped at the metal clusters. This results in a space charge stored in the bulk of the material, with a resulting field that prevents further injection. Hence, in this OFF state the conductivity is much lower than in the ON state. In the Simmons model the energy band is bent at the interface due to Fermi-level alignment. This bending confines the trapped charge in the bulk and prevents it from being released and return to the electrodes. By applying a sufficiently high voltage the trapped charge can become released again and the material is returned to the ON state. This type of switching is illustrated in figure 4.5.

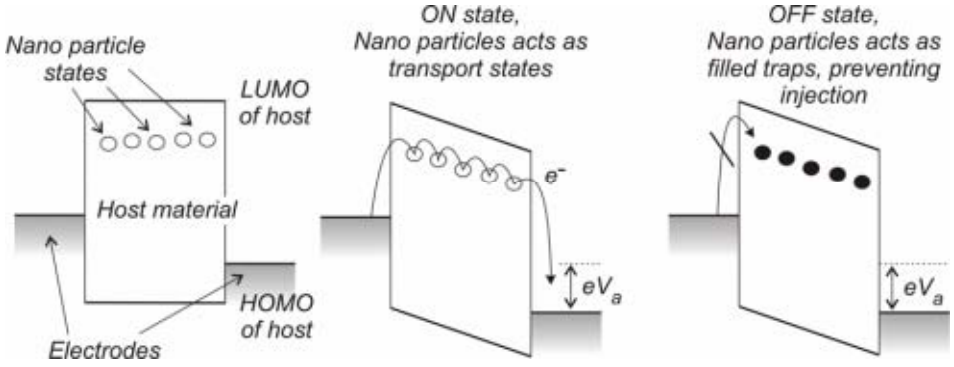

Figure 4.5: Illustration of the metal cluster switching effect. In the ON state the metal nano particles are empty and acts as transport sites. In the OFF state they are filled with trapped charge, preventing injection from the electrodes.

4.4 Extrinsic switching in organic devices

Most of the suggested organic switch devices have inorganic contacts. Typically, those contacts are either of metals that easily form oxides (*e.g.* Al) or conductive metal oxides (*e.g.* ITO). At the same time in the field of inorganic material science, a large effort is put into realizing switch devices where those very metal oxides are the active switch materials [77-82]. It is then a justified question to ask if the switching behavior observed in devices based on organic materials sandwiched in between inorganic contacts really originates in the organic layer. Recently, several studies have shown that the switching behavior in several types of organic switch devices do indeed not originate in the organic material [83-91]. Such extrinsic switching can be divided into two cases: (i) switching of the metal (oxide) electrode, or (ii) reversible growth and annihilation of metallic filaments through the organic layer.

Cölle *et al* [84] and Verbakel *et al* [90] have shown that switching in devices with similar structure as OLEDs originates in the aluminum oxide interface between the organic layer and the Al metal contact. Gomes *et al* [85] have suggested a mechanism for such resistance switching based on charge trapping in the oxide layer. In figure 4.6 the case of an electron-only device with an oxide

layer in between the organic layer and the metal electrode is shown. In the OFF state no charge is trapped in the oxide and the barrier for electron injection from the organic layer into the oxide is high. Electron transport is therefore blocked and the resistance through the device is high. As the voltage is increased sufficiently, holes are injected and become trapped in the oxide layer. As a result, space charge is built up, resulting in band bending in the oxide. Eventually, electrons can tunnel through the barrier into the oxide and the resistance becomes reduced; the device has now switched to the ON state. Since the rate of de-trapping of the holes is very low the state is quasi-stable and will be retained for long time even when no voltage is applied to the device.

The switch behavior in Cu:TCNQ-based devices has also been shown to originate from the metal oxide interface of the electrodes rather than in the organic layer [88, 91]. If the metal oxide layer is removed no switching behavior is observed. The suggested switch mechanism in this case is the electrochemical formation of highly conducting Cu paths through the metal oxide.

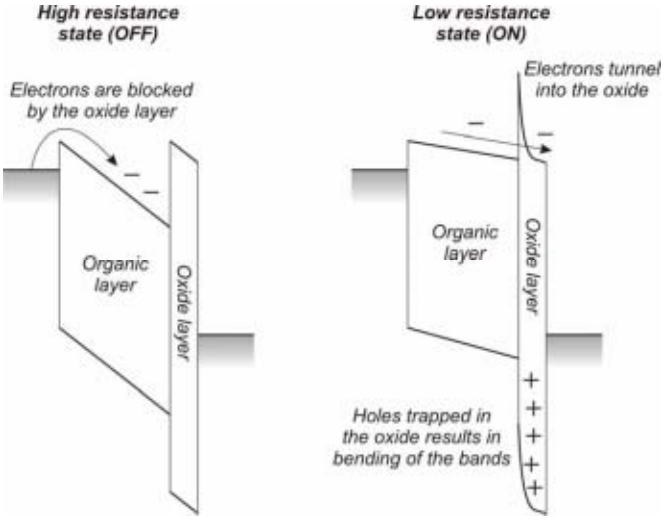

Figure 4.6: Suggested mechanism for resistance switching in devices with oxide layer in between organic layer and metal contact [85].

Switching by the reversible formation of conducting filaments through a low-conducting matrix film has been reported during the past four decades, both in inorganic [92-95] as well as in organic [96-98] materials. Several explanations for this type of switching have been proposed. In the early 70s Cook presented a model for filamentary switching based on resistive heating of the material resulting in melting or diffusion of metal atoms, causing a metallic bridge between the electrodes [99]. The temperature at the switching event has been estimated to be on the order of 1000 °C. Switching back to the off state was explained by a filament burning-off event. Hence, the reversibility of the conductivity of a specific filament is poor, but new filaments can form during subsequent switching resulting in an overall effective switching reversibility. The drawback with such devices lies in the breakdown nature of the phenomena. It is likely that this would gradually degrade the material resulting in poor endurance and also stochastic behavior. It is noteworthy that such switching should not have a polarity dependence of the applied potential. It is rather the magnitude, and not the direction, of the current that controls the switching.

Sakamoto *et al* [100, 101] reported a different model for filamentary switching observed in Cu/Cu_2S/Au devices (figure 4.7). When the Cu electrode is biased with a positive potential with respect to the Au electrode Cu^+ migrates into the Cu_2S layer, creating a metallic Cu bridge ($Cu^+ + e^- \rightarrow Cu$). When the bias is reversed the Cu ions drift back into the bottom Cu electrode resulting in a switchback to the low conductivity state.

Filamentary switching might be troublesome in a system for several reasons. Often, a very high current density is required to switch the material, which might become unfeasible as the input circuitry might not be able to generate this high input current [84]. If the filament formation cannot be well-controlled, manufacturing with high reproducibility cannot be achieved. Joo *et al* [102, 103] have investigated the latter issue by choosing the organic material carefully in order to promote filament growth [102] and by controlling the organic layer thickness in such a way that the position of the filaments can be precisely controlled [103].

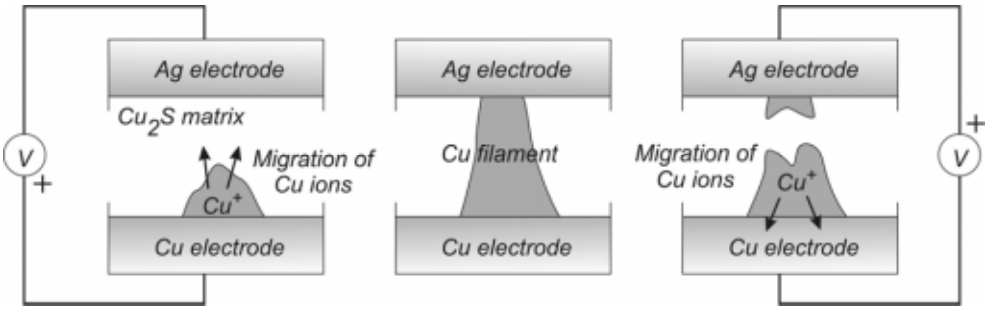

Figure 4.7. Illustration of the switching effect in Cu/Cu_2S/Au devices. To the left the Cu filament is formed by migration of Cu ions. In the middle the filament has been formed resulting in a high conductivity. To the right the filament is broken when Cu ions migrate back towards the Cu electrode.

Chapter 5

Organic electronic materials and devices

In the previous chapters the properties of organic materials have been discussed. This chapter focuses on how these materials can be used to realize devices. A wide range of organic electronic devices have been demonstrated, including organic light emitting diodes (OLED) [104-107], organic field effect transistors (OFET) [108, 109], electrochemical devices (EC) [3, 12], photovoltaics [110] and switch devices [57, 111]. In the following only OLEDs and Rose Bengal switch devices will be discussed in detail since they are of relevance to the work in this thesis.

5.1 A few examples of conjugated molecules

Figure 5.1 displays a few examples of conjugated polymers and small molecules. Two archetypal polymers are trans-polyacetylene [2] and poly(para-phenylene) [112]. While neither of them is suitable for practical applications from a stability and processability point of view, they are useful as model systems due to their relative simplicity.

The first polymer light emitting diodes used poly(para-phenylene vinylene), (PPV), as the electroluminescent layer [104, 113]. Unfortunately PPV is not easily soluble, preventing simple solution processing. However, by attaching side groups to the PPV backbone, the polymers can be made soluble. Two examples of such functionalized PPVs are poly(2-methoxy,5-(2'-ethylhexyloxy)-1,4-phenylene-vinylene), (MeH-PPV) [113], and poly(2-methoxy-5-(3',7'-dimethyloctyloxy)-1,4-phenylenevinylene, (MDMO-PPV or OC_1C_{10}-PPV) [113].

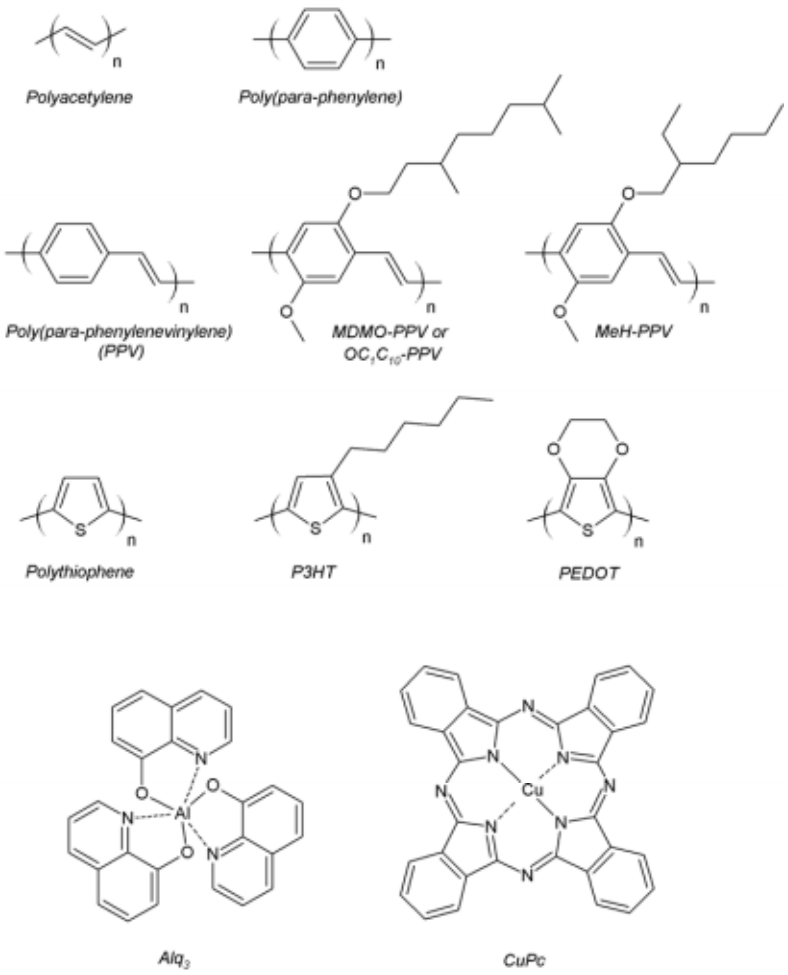

Figure 5.1: Some examples of organic polymers and small molecules

One of the most widely used conducting polymers is poly(3,4-ethylenedioxythiophene), (PEDOT), which can be doped to get a high conductivity [114, 115]. Often poly(styrene sulfonic acid), (PSS), is used as counter-doping ion. A nice side effect is that PEDOT:PSS blends forms a suspension in water, making it easy to deposit into uniform thin films. The conductivity of PEDOT-PSS can be further increased by so-called secondary doping with a small amount of some

inert solvent (*e.g.* diethylene glycol) [114]. This results in phase separation between highly conducting PEDOT:PSS and insulating excess PSS. The PEDOT:PSS-rich regions forms a interconnected network and the conductivity is increased by up to three orders of magnitude [116]

Besides polymers, there is a large selection of other smaller organic molecules used for electronic applications. Two examples are aluminum quinolate (Alq_3) [107, 113] and copper-II-phthalocyanine (CuPc) [113]. Both are used in organic light emitting diodes – Alq_3 as emitting layer and CuPc as buffer layer to improve device efficiency and lifetime.

5.2 Organic light emitting diodes

The first organic light emitting diode (OLED) was reported in 1987 by Tang *et al* [107], using Alq_3 as emitting layer, and in 1990 Burroughs *et al* [104] presented the first polymer OLED. Today, OLEDs have already reached the market in the form of small displays in household appliances, and major efforts are put into the process of commercializing large area OLED displays.

The basic device structure for a light emitting diode is shown in figure 5.2. An electroluminescent organic layer is sandwiched between a high- (anode) and a low (cathode) work function contact, at least one of them being transparent. The particular choice of work function values of the two contacts allow for easy injection of holes and electrons from the high- and low work function electrode, respectively. The oppositely charged carriers migrate towards each other in the applied field, eventually forming excitons. At least part of the excitons recombine radiatively resulting in the emission of light.

Typically, indium tin oxide (ITO) has been chosen as transparent anode. To improve surface stability and planarity a thin layer of PEDOT:PSS or similar buffer layer is commonly deposited on top of the ITO. Aluminum (Al), calcium (Ca) and magnesium (Mg) are some examples of materials that commonly are used as cathode material. The electroluminescent layer can for example consist of

MeH-PPV, MDMO-PPV or Alq_3. In figure 5.3 typical current and luminescence versus voltage data are shown.

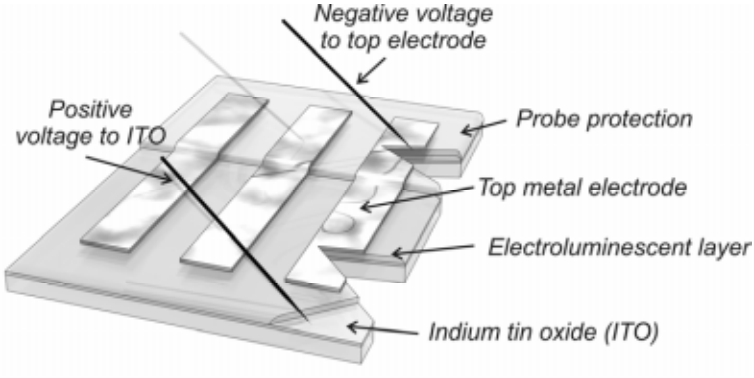

Figure 5.2: Typical structure of organic light emitting diodes. The electroluminescent layer is sandwiched between two conducting electrodes.

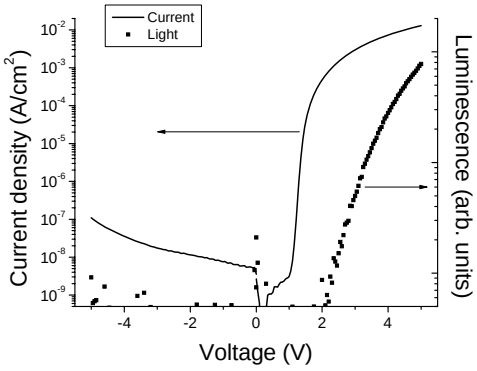

Figure 5.3: Typical current and luminescence versus voltage data for OLEDs. The device structure in this case was glass / PEDOT:PSS / MeH-PPV / Al. The PEDOT:PSS, electrode was secondarily doped with diethylene glycol to ensure high conductivity [86].

5.3 Rose Bengal switch devices

Resistance switch devices can be realized by sandwiching Rose Bengal sodium salt between ITO and Al contacts [61, 111, 117-120]. Typical J-V behavior of such devices is shown in figure 5.4. When the voltage exceeds 1.5 V the material transits to the ON state with an almost linear J-V behavior with very low resistance. When the voltage is increased above –3 V, the material is switched back to the OFF state with considerably (~200 times) higher resistance.

The switch phenomena have been attributed to the electro-reduction of the Rose Bengal molecules resulting in improved conjugation due to increased charge density on the molecule [111]. It has also been suggested that the switching is due to conformational changes of the molecule upon charging, also resulting in altered conjugation [61]. However conclusive evidence is still to be present. Paper 3 in this thesis addresses the nature of the switch behavior of Rose Bengal switch devices.

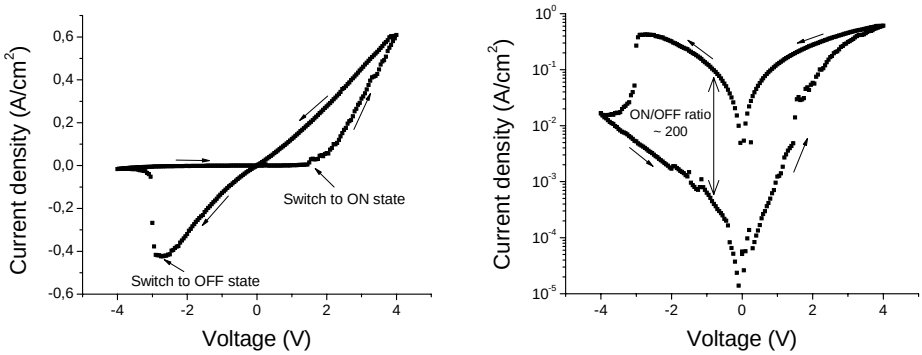

Figure 5.4: Typical Rose Bengal switch device current versus voltage behavior. To the right the data is plotted in logarithmic scale to more clearly show the difference of the current density in the ON and OFF states.

Chapter 6

Systems of resistance switch devices

In general devices do not become truly useful until they are combined into systems. In this way much more complicated tasks can be performed and the functionality of the isolated device can be enhanced. The design of inorganic based systems has been developed since the advent of the bipolar transistors in the late 1940s [121]. In the past decades the development have raced forward at a tremendous pace, following the well-known Mores law stating that the number of transistors on a chip is doubled every 18th month [122]. These systems have reached a matured state close to perfection, as is evident in everyday products such as computers and cell phones. Organic devices offer new possibilities, but also new challenges, and therefore a reassessment of traditional design paradigms might be appropriate.

Transistors have been the basic building block of electronics in the past fifty years. With the maturity of organic field effect- and electrochemical transistors, systems of low complexity have been demonstrated [3]. The drawback of transistors are that they are three terminal devices, requiring routing of three lines to each device for proper operation. With two-terminal devices less complicated designs can be realized, thus taking full advantage of the low cost manufacturability of organic materials. An example of a very simple system for two-terminal devices is the cross-point array, also called passive matrix or crossbar circuit, see figure 6.1. It consists of an active material sandwiched between two sets of crossing lines, where each crossing defines a device. This kind of design can be used for display-, sensor-, memory- as well as logic circuits [123-125]. Cross-point arrays have also been studied and considered for use in molecular electronics since it offers extremely high device densities [124, 126]. In

this thesis one focus is switch devices in cross-point arrays for memory applications.

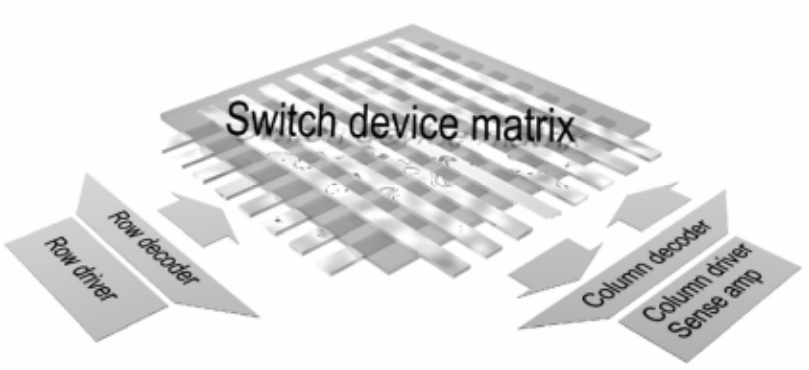

Figure 6.1: A cross-point array consists of an active material sandwiched between two orthogonal sets of lines. Circuitry for addressing and sensing is located outside of the array.

6.1 Addressing

Each individual device needs to be uniquely addressable in order to set (write) or probe (read) the state of the material. This can be achieved by applying the potentials on the top and bottom lines in a certain manner. Three different addressing schemes are shown in figure 6.2. With the V2 addressing scheme the potentials on the addressed row and column is V/2 and -V/2 respectively, while the potential on all other lines are 0 V. In this way the addressed cross-point experiences the voltage V required for operation. Even though most unaddressed cross-points experience no voltage, all unaddressed cross-points along the addressed row and column also experience a disturbing voltage of ±V/2. Therefore it is important that the switch material can retain its state when disturbed by such a voltage.

A way to reduce the magnitude of the disturb voltage is to use the V3 addressing scheme [127]. In this scheme a potential of V and 0 are applied to the addressed row and column, respectively, while a potential of V/3 and 2V/3 is

applied to the unaddressed rows and columns respectively. Hence, the addressed cross-point will experience the voltage V, while all unaddressed cross-points experience a voltage of only ±V/3. In order to perform an operation (read or write) on each cross-point in an array of M columns and N rows once, all devices will experience N x M disturbs using the V3 scheme compared to only M + N – 1 for the V2 scheme. The choice of addressing method therefore depends on what is best for the material: few high-magnitude disturb signals or many low-magnitude disturb signals.

In virtual ground sense (VGS) [124, 128] scheme the addressed row have a potential of V while all other lines have zero potential. In this way all cross-points along the addressed row experience the voltage V and hence all of them are addressed simultaneously. However, no other cross-points experience a voltage so there is no disturb issue. Another advantage is that since only the addressed row has a non-zero voltage (ideally) no leakage current from unaddressed rows will contribute to the current into the sense amplifiers. However, VGS cannot be used to address individual cross-points along the row, and therefore it is limited to read operations. Note also that in general a lower voltage can be used for read than for write operation, further reducing the problem with disturb signals for read operations.

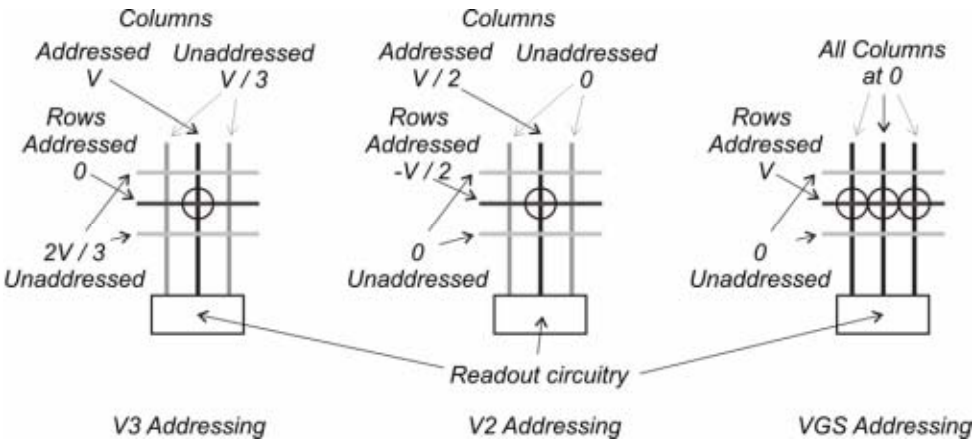

Figure 6.2: V3- (left), V2- (middle) and VGS (right) addressing schemes.

6.2 A model for cross-point arrays

In the static case the cross-point array can be represented by a resistance network with a line resistance of R_w, a resistance R_a and R_{ua} through addressed- and unaddressed cross-points and M and N number of columns and rows respectively, see figure 6.3. Two equations describes each cross point – one for the net current into the top line and one for the net current out of the bottom line of the cross-point. The system is then described by 2 x M x N interconnected equations, making simulations cumbersome even for modest sized arrays. A simplified model that allows for much less demanding calculations, has been suggested by Ziegler *et al* [129] (right in figure 6.3). In this model the line resistance is lumped together to a resistance at the beginning of the line. As a result all unaddressed rows and columns can be regarded as identical parallel circuits and can be lumped together into two equivalent resistances. This model will give a worst case for calculations of the potential drop along the lines. For simplicity the line resistance of the columns and the rows can be assumed to be the same.

In reality the resistance through each cross-point will depend on what state the material is in (ON or OFF) and might also be field-dependent. For simplicity, the resistance behavior of the switch device can be modeled with three resistance levels (figure 6.4) – the resistance of the addressed devices in the two different states, $R_{a,ON}$ and $R_{a,OFF}$, and the resistance of the unaddressed devices, R_{ua}. The ratio, r_0, between $R_{a,ON}$ and $R_{a,OFF}$ is denoted the ON/OFF ratio. The J-V behavior of switch devices is often linear, i.e. ohmic, in at least one of the states. This is for example the case for Rose Bengal switch devices in the ON state. For such devices R_{ua} is simply the same as R_a. A non-linear J-V behavior, as in organic diodes, can be incorporated into the model by setting $R_{ua} = kR_a$. For simplicity it is assumed that all unaddressed cross-points have the same resistance, i.e. that all unaddressed cross-points are in the ON state. Another simplification is that the J-V behavior is assumed to be symmetric, i.e. the devices are non-rectifying.

Typical resistance for a Rose Bengal switch device in the ON state with an active area of $1\mu m^2$ is 500 MΩ. The ON/OFF ratio for these devices is usually $r_0 \sim 100$. It is reasonable to assume that the sheet resistance, R_w, for lithographically

defined metal lines is near 1 Ω/□. For organic conductors the sheet resistance will most likely be much higher. The sheet resistance of PEDOT:PSS can be as low as 100 Ω/□.

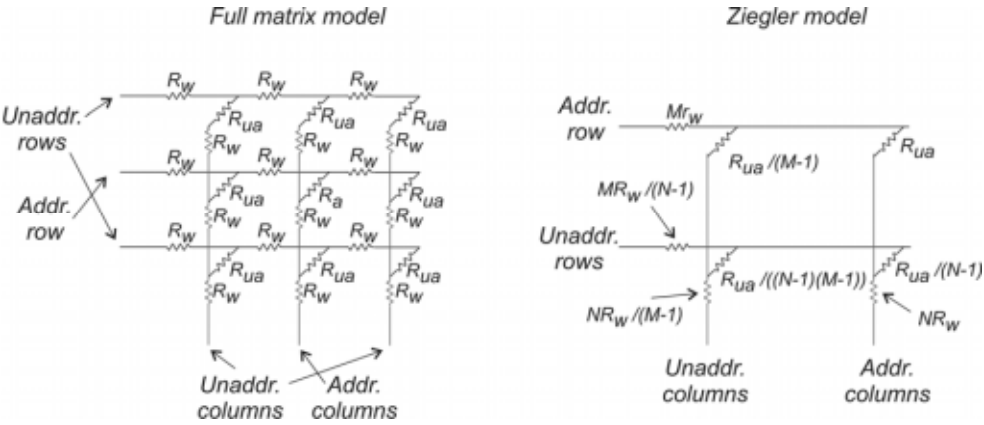

Figure 6.3: The array can be represented by a resistance network (left). The Ziegler model (right) simplifies the computation of the behavior of the array. This model can be used for V2- and V3 addressing schemes, but has to be slightly modified for VGS addressing.

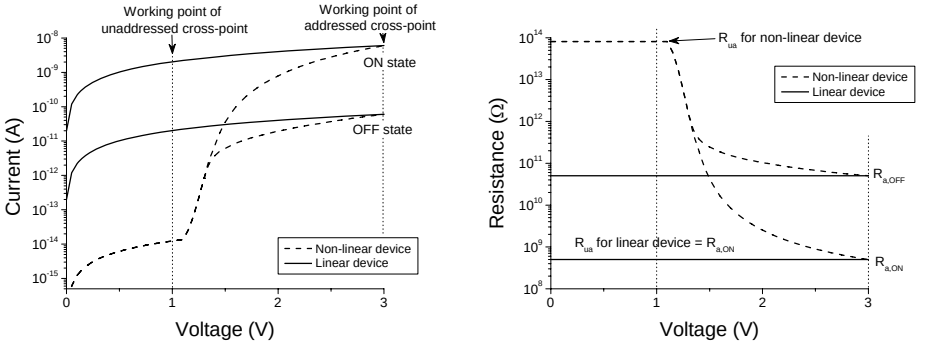

Figure 6.4: The resistance levels of the device can be modeled by three discrete resistance levels – the resistance of the addressed cross-point in the ON state ($R_{a,ON}$) and in the off state ($R_{a,OFF}$), and the resistance of the unaddressed cross-point (R_{ua}).

6.3 Potential drop along lines

Due to a finite line resistance there will be a potential drop along the lines. The magnitude of the drop depends on addressing scheme, is proportional to the line resistance and inversely proportional to the resistance through the cross-points. This gives that if the ratio between the line resistance and the cross-point resistance is high, the potential drop can be significant, resulting in a lower than nominal voltage across the cross-points. This can be a problem since the voltage across the device is important for its behavior. Even though a small perturbation from the nominal voltage is not very crucial a larger perturbation might cause the addressed device to switch only partly or disturb unaddressed cross-points more than desired.

In figure 6.5, the simulated voltage across the end cross-point on the addressed row is shown in the case of V2 addressing of linear devices with a resistance in the ON state of 500 MΩ and an ON/OFF ratio of 100. As the line resistance is increased the drop of the potential is shifted towards smaller arrays (i.e. fewer rows). It is reasonable to assuming that a voltage of at least 90% of the nominal value (dotted line) is required for proper device operation. With this requirement it is possible to realize an array of 16 Mbit (4096 by 4096 lines) using lines with a line resistance of 1 Ω/□. If the line resistance is increased to 100 Ω/□ the larges array size is reduced to 256 kbit (512 by 512 lines).

In figure 6.6, dependence of the potential drop on resistance through the addressed cross-point is shown. In this case the line resistance is 100 Ω/□. Decreasing the cross-point resistance makes the potential drop more severe. Using a non-linear device the current through the unaddressed cross-points will be reduced, hence reducing the total current through the lines. This will reduce the potential drop significantly as is evident from figure 6.6. With a line resistance of 100 Ω/□ and a resistance through the addressed cross-point of 500 MΩ the largest array size can be increased from 16 kbit (512 by 512 lines) to 16 Mbit (4096 x 4096 lines) by going from linear devices to devices with a non-linearity equivalent to k = 100.

The results for V3 addressing are similar. Using VGS addressing however, non-linearity has a limited effect since all cross-points along the addressed row is

simultaneously addressed. Hence, the voltage across all the cross-points along the addressed row will be high and a large current will pass through them.

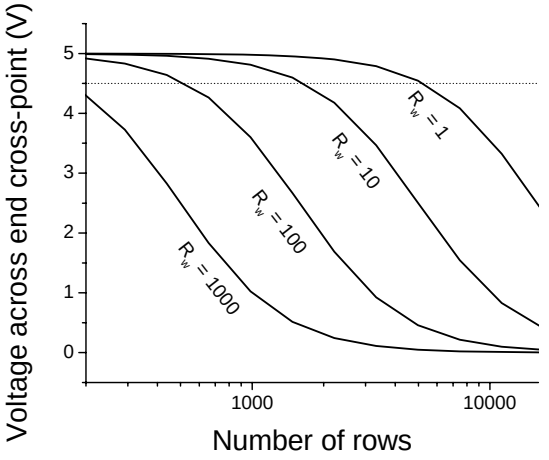

Figure 6.5: Simulation of the voltage at the end cross-point of an array versus array size. The number of rows and columns are the same. Resistance through addressed cross-point is R_a = 500 MΩ and the line resistance values are given next to the curves in Ω/□. V2 addressing scheme is used and the drive voltage is 5 V.

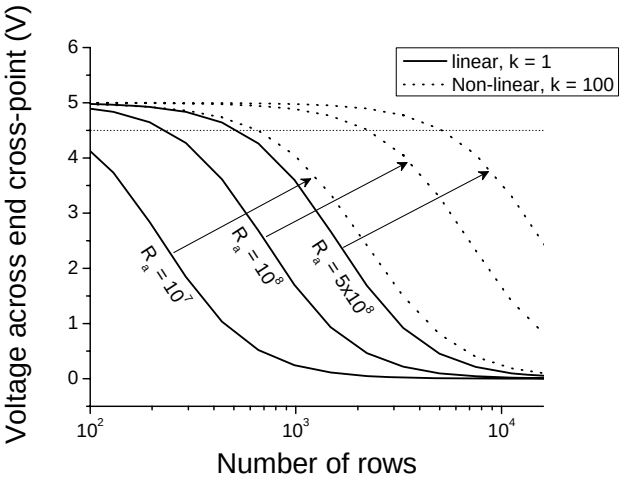

Figure 6.6: Simulation of the voltage at the end cross-point of an array versus array size. The number of rows and columns are the same. Line resistance is 100 Ω/□, comparable to conducting polymers such as PEDOT:PSS. The resistance of the addressed cross-points is given in the figure. V2 addressing scheme is used and the drive voltage is 5 V.

6.4 Sense current from the addressed cross-point

In order to determine whether a cross-point is in the ON- or OFF state the difference of the current in both states have to be large enough with respect to noise and leakage contribution from unaddressed cross-points. An effective ON/OFF ratio, r_{eff}, can be defined as the ratio between the current out from the addressed column in state ON and OFF. This will deviate from the ON/OFF ratio of the isolated device, r_0, due to contribution to the ON and OFF currents from unaddressed cross-points. In figure 6.7 the effective ON/OFF ratio is plotted as a function of array size, for V2-, V3 and VGS addressing schemes. The addressed cross-point resistance is 500 MΩ, line resistance 1 Ω/□ and r_0 is 100. As is evident VGS is superior to V2 and V3, with r_{eff} close to r_0 as long as the array is not humongous ($r_{eff} \approx 0.5\ r_0$ for a 256 Mbit array). Since all columns and unaddressed rows are kept at zero potential, very little leakage current contributes to the sense signal. Neither is r_{eff} affected by nonlinearity in the device J-V behavior for the same reason.

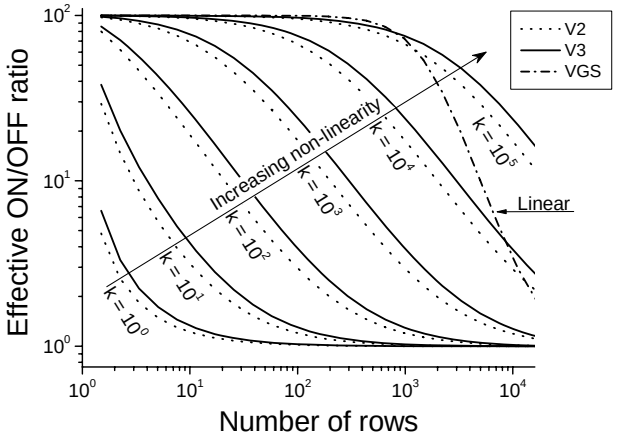

Figure 6.7: Simulation of the effective ON/OFF ratio for varying device nonlinearity. The number of rows and columns are the same. The resistance through addressed cross-point is R_a = 500 MΩ and the line resistance is 1 Ω/□. The nonlinearity factor of the devices is shown next to the curves. Only data for the case of a linear device is shown for VGS since nonlinearity has no impact on VGS readout.

When using V2 or V3 addressing schemes each unaddressed cross-point on the addressed column contributes to the readout current with a significant leakage current, particularly when using linear devices. As can be seen in figure 6.7 r_{eff} is very small even for small arrays if the nonlinearity is not increased. Practical array sizes requires a nonlinearity exceeding $k = 10^3$.

References

[1] T. Frängsmyr, *Les Prix Nobel - The Nobel Prizes 2000*, Almqvist & Wiksell international, Stockholm, 2001.

[2] C. K. Chiang, C. R. Fincher Jr., Y. W. Park, A. J. Heeger, H. Shirakawa, E. J. Louis, S. C. Gau and A. G. MacDiarmid, Phys. Rev. Lett. 39 (1977) 1098.

[3] D. Nilsson, N. D. Robinson, M. Berggren and R. Forchheimer, Adv. Mater. 17 (2005) 353.

[4] M. A. Reed, J. Chen, A. M. Rawlett, D. W. Price and J. M. Tour, Appl. Phys. Lett. 78 (2001) 3735.

[5] R. A. van Delden, M. K. J. ter Wiel, M. M. Pollard, J. Vicario, N. Koumura and B. L. Feringa, Nature 437 (2005) 1337.

[6] J. H. Fendler, Chem. Mater. 13 (2001) 3196.

[7] P. Atkins and J. de Paula, *Physical Chemistry*, Oxford University Press, Oxford, 2002.

[8] T. A. Skotheim, R. L. Elsenbaumer and J. R. Reynolds, *Handbook of Conducting Polymers*, MARCEL DEKKER, INC, New York, 1998.

[9] M. Pope and C. E. Swenberg, *Electronic Processes in Organic Crystals and Polymers*, Oxford University Press, New York, 1999.

[10] A. Moliton and R. C. Hiorns, Polymer Int. 53 (2004) 1397.

[11] W. P. Su, J. R. Schrieffer and A. J. Heeger, Phys. Rev. B 22 (1980) 2099.

[12] D. Nilsson, M. Chen, T. Kugler, T. Remonen, M. Armgarth and M. Berggren, Adv. Mater. 14 (2002) 51.

[13] C. J. Cramer, *Essentials of Computational Chemistry*, John Wiley & Sons, Ltd, Chichester, 2004.

[14] R. O. Jones and O. Gunnarsson, Rev. Mod. Phys. 61 (1989) 689.

[15] W. Kohn, A. D. Becke and R. G. Parr, J. Phys. Chem. 100 (1996) 12974.

[16] S. F. Sousa, P. A. Fernandes and M. J. Ramos, J. Phys. Chem. A 111 (2007) 10439.

[17] P. Hohenberg and W. Kohn, Phys. Rev. 136 (1964) B864.

[18] W. Kohn and L. J. Sham, Phys. Rev. 140 (1965) A1133.

[19] N. W. Ashcroft and N. D. Mermin, *Solid State Physics*, Thomson Learning, Inc., 1976.

[20] K. W. Böer, *Survey of Semiconductor Physics,* John Wiley & Sons, Inc., New York, 2002.

[21] H. Bässler, Phys. Stat. Sol. (b) 175 (1993) 15.

[22] A. Dieckmann, H. Bässler and P. M. Borsenberger, J. Chem. Phys. 99 (1993) 8136.

[23] D. H. Dunlap, P. E. Parris and V. M. Kenkre, Phys. Rev. Lett. 77 (1996) 542.

[24] S. V. Novikov and G. G. Malliaras, Phys. Rev. B 73 (2006) 033308.

[25] S. V. Novikov and A. V. Vannikov, Mol. Cryst. Liq. Cryst. Sci. Technol., Sect. A 361 (2001) 89.

[26] R. H. Young, Phil. Mag. B 72 (1995) 437.

[27] Y. N. Gartstein and E. M. Conwel, Chem. Phys. Lett. 245 (1995) 351.

[28] S. V. Novikov, D. H. Dunlap, V. M. Kenkre, P. E. Parris and A. V. Vannikov, Phys. Rev. Lett. 81 (1998) 4472.

[29] S. V. Novikov and G. G. Malliaras, Phys. Rev. B 73 (2006) 033302.

[30] P. F. Barbara, T. J. Meyer and M. A. Ratner, J. Phys. Chem. 100 (1996) 13148.

[31] J.-L. Brédas, D. Beljonne, V. Coropceanu and J. Cornil, Chem. Rev. 104 (2004) 4971.

[32] S. F. Baranovskii, T. Faber, F. Hensel and P. Thomas, J. Phys: Cond. Matt. 9 (1997) 2699.

[33] R. Coehoorn, W. F. Pasveer, P. A. Bobbert and M. A. J. Michels, Phys. Rev. B 72 (2005) 155206.

[34] W. F. Pasveer, J. Cottaar, C. Tanase, R. Coehoorn, P. A. Bobbert, P. W. M. Blom, D. M. de Leeuw and M. A. J. Michels, Phys. Rev. Lett. 94 (2005) 206601.

[35] V. I. Arkhipov, H. von Seggern and H. V. Emelianova, Appl. Phys. Lett. 83 (2003) 5074.

[36] U. Wolf, S. Barth and H. Bässler, Appl. Phys. Lett. 75 (1999) 2035.

[37] G. G. Malliaras, J. R. Salem, P. J. Brock and C. Scott, Phys. Rev. B 58 (1998) R13411.

[38] P. N. Murgatroyd, J. Phys. D 3 (1970) 151.

[39] G. G. Malliaras, J. R. Salem, P. J. Brock and J. C. Scott, J. Appl. Phys. 84 (1998) 1583.

[40] X. Wei, S. A. Jeglinski and Z. V. Vardeny, Synth. Met. 85 (1997) 1215.

[41] X. Wei, M. Raikh and Z. V. Vardeny, Phys. Rev. B 49 (1994) 17480.

[42] V. I. Arkhipov, E. V. Emelianova, Y. H. Tak and H. Bässler, J. Appl. Phys. 84 (1998) 848.

[43] M. A. Baldo and S. R. Forrest, Phys. Rev. B 64 (2001) 085201.

[44] L. A. Burin and M. A. Ratner, J. Pol. Sci. B 41 (2003) 2601.

[45] V. I. Arkhipov, U. Wolf and H. Bässler, Phys. Rev. B 59 (1999) 7514.

[46] U. Wolf, V. I. Arkhipov and H. Bässler, Phys. Rev. B 59 (1999) 7507.

[47] D. F. Blossey, Phys. Rev. B 9 (1974) 5183.

[48] L. Onsager, Phys. Rev. 54 (1938) 554.

[49] W. Osikowicz, X. Crispin, C. Tengstedt, L. Lindell, T. Kugler and W. R. Salaneck, Appl. Phys. Lett. 85 (2004) 1616.

[50] L. Lindell, M. P. de Jong, W. Osikowicz, R. Lazzaroni, M. Berggren, W. R. Salaneck and X. Crispin, J. Chem. Phys. 122 (2005) 084712.

[51] L. Lindell, A. Burquel, F. L. E. Jakobsson, V. Lemaur, M. Berggren, R. Lazzaroni, J. Cornil, W. R. Salaneck and X. Crispin, Chem. Mater. 18 (2006) 4246.

[52] X. Crispin, V. Geskin, A. Crispin, J. Cornil, R. Lazzaroni, W. R. Salaneck and J. L. Brédas, J. Am. Chem. Soc. 124 (2002) 8131.

[53] P. W. M. Blom and M. C. J. M. Vissenberg, Mat. Sci. Eng. 27 (2000) 53.

[54] S. Möller, C. Perlov, W. Jackson, C. Taussig and S. R. Forrest, Nature 426 (2003) 166.

[55] J. C. Scott and L. D. Bozano, Adv. Mater. 19 (2007) 1452.

[56] R. Pati and S. Karna, Phys. Rev. B 69 (2004) 155419.

[57] P. Andersson, N. D. Robinson and M. Berggren, Adv. Mater. 17 (2005) 1798.

[58] T. Tsujioka and K. Masuda, Appl. Phys. Lett. 83 (2003) 4978.

[59] S. Nešpůrek and J. Sworakowski, Thin Solid Films 393 (2001) 168.

[60] S. Nešpůrek, J. Sworakowski, C. Combellas, G. Wang and M. Weiter, Appl. Surf. Sci. 234 (2004) 395.

[61] A. Bandyopadhyay and A. J. Pal, Appl. Phys. Lett. 84 (2004) 999.

[62] R. Kumai, Y. Okimoto and Y. Tokura, Science 284 (1999) 1645.

[63] C. Sato, S. Wakamatsu, K. Tadokoro and K. Ishii, J. Appl. Phys. 68 (1990) 6535.

[64] J. B. Torrance, J. E. Vazquez, J. J. Mayerle and V. Y. Lee, Phys. Rev. Lett. 46 (1981) 253.

[65] J. Hubbard and J. B. Torrance, Phys. Rev. Lett. 47 (1981) 1750.

[66] R. S. Potember, T. O. Poehler and D. O. Cowan, Appl. Phys. Lett. 34 (1979) 405.

[67] R. S. Potember, T. O. Poehler and R. C. Benson, Appl. Phys. Lett. 41 (1982) 548.

[68] R. Müller, S. de Jonge, K. Myny, D. J. Wouters, J. Genoe and P. Heremans, Sol. Stat. Elec. 50 (2006) 601.

[69] J. G. Simmons and R. R. Verderber, Proc. Roy. Soc. London A 301 (1967) 77.

[70] L. Ma, J. Liu, S. Pyo and Y. Yang, Appl. Phys. Lett. 80 (2002) 362.

[71] L. Ma, Q. Xu and Y. Yang, Appl. Phys. Lett. 84 (2004) 4908.

[72] L. P. Ma, J. Liu and Y. Yang, Appl. Phys. Lett. 80 (2002) 2997.

[73] J. Ouyang, C.-W. Chu, C. R. Szmanda, L. Ma and Y. Yang, Nature Mater. 3 (2004) 918.

[74] L. D. Bozano, B. W. Kean, M. Beinhoff, K. R. Carter, P. M. Rice and J. C. Scott, Adv. Func. Mater. 15 (2005) 1933.

[75] H. S. Majumdar, J. K. Baral, R. Österbacka, O. Ikkala and H. Stubb, Organ. El. 6 (2005) 188.

[76] J. K. Baral, H. S. Majumdar, A. Laiho, H. Jiang, E. I. Kauppinen, R. H. A. Ras, J. Ruokolainen, O. Ikkala and R. Österbacka, Nanotechnology 19 (2008) 035203.

[77] A. Beck, J. G. Bednorz, C. Gerber, C. Rossel and D. Widmer, Appl. Phys. Lett. 77 (2000) 139.

[78] B. J. Choi, D. S. Jeong, S. K. Kim, C. Rhode, S. Choi, J. H. Oh, H. J. Kim, C. S. Hwang, K. Szot, R. Waser, B. Reichenberg and S. Tiedke, J. Appl. Phys. 98 (2005) 033715.

[79] R. Dong, D. S. Lee, W. F. Xiang, S. J. Oh, D. J. Seong, S. H. Heo, H. J. Choi, M. J. Kwon, S. N. Seo, M. B. Pyun, M. Hasan and H. Hwang, Appl. Phys. Lett. 90 (2007) 042107.

[80] O. Kurnosikov, F. C. de Nooij, P. LeClair, J. T. Kohlhepp, B. Koopmans, H. J. M. Swagten and W. J. M. de Jonge, Phys. Rev. B 64 (2001) 153407.

[81] K. Szot, R. Dittmann, W. Speier and R. Waser, Phys. Stat. Sol. (RRL) 1 (2007) R86.

[82] S. Tsui, A. Baikalov, J. Cmaidalka, Y. Y. Sun, Y. Q. Wang, Y. Y. Xue, C. W. Chu, L. Chen and A. J. Jacobson, Appl. Phys. Lett. 85 (2004) 317.

[83] L. Chen, Y. Xia, X. Liang, K. Yin, J. Yin and Z. Liu, Appl. Phys. Lett. 91 (2007) 073511.

[84] M. Cölle, M. Büchel and D. M. de Leeuw, Organ. El. 7 (2006) 305.

[85] H. L. Gomes, A. R. V. Benvenho, D. M. de Leeuw, M. Cölle, P. Stallinga, F. Verbakel and D. M. Taylor, Organ. El. 9 (2008) 119.

[86] F. L. E. Jakobsson, X. Crispin, M. Cölle, M. Büchel, D. M. de Leeuw and M. Berggren, Organ. El. 8 (2007) 559.

[87] S. Karthäuser, B. Lüssem, M. Weides, M. Alba, A. Besmehn, R. Oligschlaeger and R. Waser, J. Appl. Phys. 100 (2006) 094504.

[88] T. Kever, U. Böttger, C. Schindler and R. Waser, Appl. Phys. Lett. 91 (2007) 083506.

[89] D. R. Stewart, D. A. A. Ohlberg, P. A. Beck, Y. Chen, R. Stanley Williams, J. O. Jeppesen, K. A. Nielsen and J. Fraser Stoddart, Nano letters 4 (2004) 133.

[90] F. Verbakel, S. C. J. Meskers and R. A. J. Janssen, Appl. Phys. Lett. 91 (2007) 192103.

[91] J. Billen, S. Steudel, R. Müller, J. Genoe and P. Heremans, Appl. Phys. Lett. 91 (2007) 263507.

[92] Y. Kawamura, Y. Kashiwaba and T. Ikeda, Jpn. J. Appl. Phys. 21 (1982) 429.

[93] M. Shatzkes, M. Av-Ron and R. M. Anderson, J. Appl. Phys. 45 (1974) 2065.

[94] A. G. Steventon, J. Phys. D 8 (1975) 120.

[95] D. F. Weirauch, Appl. Phys. Lett. 16 (1970) 72.

[96] L. F. Pender and R. J. Fleming, J. Appl. Phys. 46 (1975) 3426.

[97] Y. Segui, B. Ai and H. Carchano, J. Appl. Phys. 47 (1976) 140.

[98] H. Carchano, R. Lacoste and Y. Segui, Appl. Phys. Lett. 19 (1971) 414.

[99] E. L. Cook, J. Appl. Phys. 41 (1970) 551.

[100] S. Kaeriyama, T. Sakamoto, H. Sunamura, M. Mizuno, H. Kawaura, T. Hasegawa, K. Terabe, T. Nakayama and M. Aono, IEEE J. Sol. Stat. Circ. 40 (2005) 168.

[101] T. Sakamoto, H. Sunamura, H. Kawaura, T. Hasegawa, T. Nakayama and M. Aono, Appl. Phys. Lett. 82 (2003) 3032.

[102] W.-J. Joo, T.-L. Choi, J. Lee, S. K. Lee, M.-S. Jung, N. Kim and J. M. Kim, J. Phys. Chem. B 110 (2006) 23812.

[103] W.-J. Joo, T.-L. Choi and K.-H. Lee, Thin Solid Films 516 (2008) 3133.

[104] J. H. Burroughes, D. D. C. Bradley, A. R. Brown, R. N. Marks, K. Mackay, R. H. Friend, P. L. Burns and A. B. Holmes, Nature 347 (1990) 539.

[105] R. H. Friend, Pure Appl. Chem. 73 (2001) 425.

[106] W. R. Salaneck, R. H. Friend and J.-L. Brédas, Phys. Rep. 319 (1999) 231.

[107] C. W. Tang and S. A. VanSlyke, Appl. Phys. Lett. 51 (1987) 913.

[108] G. Horowitz, Adv. Mater. 10 (1998) 365.

[109] A. Tsumura, H. Koezuka and T. Ando, Appl. Phys. Lett. 49 (1986) 1210.

[110] N. S. Sariciftci, L. Smilowitz, A. J. Heeger and F. Wudl, Science 258 (1992) 1474.

[111] A. Bandhopadhyay and A. J. Pal, J. Phys. Chem. B 107 (2003) 2531.

[112] W. J. Feast, J. Tsibouklis, K. L. Pouwer, L. Groenendaal and E. W. Meijer, Polymer 37 (1996) 5017.

[113] U. Mitschke and P. Bäuerle, J. Mat. Chem. 10 (2000) 1471.

[114] X. Crispin, S. Marciniak, W. Osikowicz, G. Zotti, A. W. Denier vad der Gon, F. Louwet, M. Fahlman, L. B. Groenendaal, F. de Schryver and W. R. Salaneck, J. Pol. Sci. B 41 (2003) 2561.

[115] L. B. Groenendaal, F. Jonas, D. Freitag, H. Pielartzik and J. R. Reynolds, Adv. Mater. 12 (2000) 481.

[116] X. Crispin, F. L. E. Jakobsson, A. Crispin, P. C. M. Grim, P. Andersson, A. Volodin, C. van Haesendonck, M. Van der Auweraer, W. R. Salaneck and M. Berggren, Chem. Mater. 18 (2006) 4354.

[117] A. Bandhopadhyay and A. J. Pal, J. Phys. Chem. B 109 (2005) 6084.

[118] A. Bandyopadhyay and A. J. Pal, Chem. Phys. Lett. 371 (2003) 86.

[119] A. Bandyopadhyay and A. J. Pal, Appl. Phys. Lett. 82 (2003) 1215.

[120] S. K. Majee, A. Bandyopadhyay and A. J. Pal, Chem. Phys. Lett. 399 (2004) 284.

[121] J. Bardeen and W. H. Brattain, Phys. Rev. 74 (1948) 230.

[122] G. E. Moore, Electronics 38 (1965) 114.

[123] C. J. Amsinck, N. H. Di Spigna, D. P. Nackashi and P. D. Franzon, Nanotechnology 16 (2005) 2251.

[124] R. J. Luyken and F. Hofmann, Nanotechnology 14 (2003) 273.

[125] D. Pribat and F. Plais, Thin solid films 383 (2001) 25.

[126] Y. Chen, G.-Y. Jung, D. A. A. Ohlberg, X. Li, D. R. Stewart, J. O. Jeppesen, K. A. Nielsen, J. F. Stoddart and R. S. Williams, Nanotechnology 14 (2003) 462.

[127] J. Tannas, *One-third selection scheme for addressing a ferroelectric matrix arrangement*, U.S. Patent No. 4 169 258 (May 15 1978).

[128] T. Ramcke, L. Risch and W. Roesner, *Memory cell configuration, magnetic RAM, and associative memory*, U.S. Patent No. 6 490 190 B1 (Dec 3 2002).

[129] M. M. Ziegler and M. R. Stan, IEEE Trans. Nanotech. 2 (2003) 217.